Voltage-dependent K$^+$ Currents and Underlying Single K$^+$ Channels in Pheochromocytoma Cells

TOSHINORI HOSHI and RICHARD W. ALDRICH

From the Department of Neurobiology, Stanford University School of Medicine, Stanford, California 94305

ABSTRACT   Properties of the whole-cell K$^+$ currents and voltage-dependent activation and inactivation properties of single K$^+$ channels in clonal pheochromocytoma (PC-12) cells were studied using the patch-clamp recording technique. Depolarizing pulses elicited slowly inactivating whole-cell K$^+$ currents, which were blocked by external application of tetraethylammonium$^+$, 4-aminopyridine, and quinidine. The amplitudes and time courses of these K$^+$ currents were largely independent of the prepulse voltage. Although pharmacological agents and manipulation of the voltage-clamp pulse protocol failed to reveal any additional separable whole-cell currents in a majority of the cells examined, single-channel recordings showed that, in addition to the large Ca^{++}-dependent K$^+$ channels described previously in many other preparations, PC-12 cells had at least four distinct types of K$^+$ channels activated by depolarization. These four types of K$^+$ channels differed in the open-channel current-voltage relation, time course of activation and inactivation, and voltage dependence of activation and inactivation. These K$^+$ channels were designated the K$_W$, K$_Z$, K$_Y$, and K$_X$ channels. The typical chord conductances of these channels were 18, 12, 7, and 7 pS in the excised configuration using Na$^+$-free saline solutions. These four types of K$^+$ channels opened in the presence of low concentrations of internal Ca^{++} (1 nM). Their voltage-dependent gating properties can account for the properties of the whole-cell K$^+$ currents in PC-12 cells.

INTRODUCTION

Voltage-dependent gating of K$^+$ channels has been studied extensively in various preparations using macroscopic voltage-clamp techniques (for review, see Thompson and Aldrich, 1980). These studies have suggested that there are multiple kinetically and pharmacologically distinct populations of voltage-dependent K$^+$ channels, such as A-currents and delayed rectifier currents, and that these K$^+$ channels have several nonconductive (closed) and conductive (open) states, resulting in complex whole-cell K$^+$ currents. The single-channel recording method (Hamill et al., 1981) has also been used to investigate gating properties of K$^+$ channels. A great deal of information is now available on the steady state

gating properties of some K^+ channels (for review, see Latorre et al., 1984). However, nonstationary gating properties of the voltage-dependent K^+ channels have not been thoroughly investigated.

Clonal pheochromocytoma (PC-12) cells, derived from chromaffin cells of rat adrenal medulla, are a good model system for studies of regulation of neuronal excitability. Voltage-dependent K^+ channels in undifferentiated PC-12 cells can be studied using both the whole-cell and single-channel recording methods. Biochemical events in PC-12 cells, such as those involving cyclic nucleotides and Ca^{++}, have been studied extensively, making these cells suitable for the study of short-term regulation of neuronal excitability. PC-12 cells are also well suited for the study of long-term regulation of neuronal excitability. PC-12 cells can undergo differentiation upon application of nerve growth factor (NGF) to develop properties characteristic of sympathetic ganglion neurons (Greene and Tischler, 1976). In addition to the morphological changes, the differentiation involves changes in the properties of voltage-dependent Na^+ channels and acetylcholine receptor channels (Dichter et al., 1977) and probably some K^+ channels (Schmid-Antomarch et al., 1986).

In this and the accompanying article (Hoshi and Aldrich, 1988), we present a systematic analysis of the voltage-dependent K^+ channels in PC-12 cells. This paper focuses on two major issues: (a) the properties of the whole-cell K^+ currents, and (b) the time course and voltage dependence of the activation and inactivation of single K^+ channels that underlie the whole-cell currents. Detailed descriptions of gating properties of these voltage-dependent K^+ channels are presented in the following article.

MATERIALS AND METHODS

Cell Culture

PC-12 cells were obtained from the laboratory of Prof. E. M. Shooter, Stanford University, Stanford, CA. The cells were grown without NGF in Dulbecco's modified Eagle's medium (DMEM) supplemented with 5% bovine calf serum (Hyclone Laboratories, Logan, UT) and 5% horse serum (Hyclone Laboratories). In later experiments, the cells were grown in DMEM with 25 mM HEPES supplemented with 10% calf serum (Gibco Laboratories, Grand Island, NY). The cells were normally maintained in plastic culture dishes (Falcon Plastics, Oxnard, CA, or Miles Scientific, Naperville, IL) and then plated on glass coverslips 1–14 d before use. We did not see any obvious differences in the electrophysiological properties of PC-12 cells grown in these two different culture media.

Electrophysiology

Experiments were performed using an LSI 11/73-based (Digital Equipment Corp., Maynard, MA) minicomputer system (Indec Systems, Sunnyvale, CA). The output of the patch-clamp amplifier (Yale Mk V, Physiology Dept. Electronics Shop, Yale University School of Medicine, New Haven, CT, or List EPC-7, List-Medical Systems, Greenvale, NY) was low-pass-filtered through an eight-pole Bessel filter (Frequency Devices, Inc., Haverhill, MA) and digitized at the frequencies indicated in the figure legends. In some cases, digitized data were further filtered using the Gaussian digital filter routine described in Colquhoun and Sigworth (1983).

The junction potential was nulled immediately before the seal was made in both whole-

cell and single-channel recordings. Judging from the reversal potentials of the whole-cell K^+ currents and single K^+ channels recorded using symmetrical K^+ solutions, the voltage error caused by the junction potential was estimated to be <5 mV. The voltages referred to in this and the accompanying article are not corrected for the error.

Whole-cell recording. Spherical PC-12 cells of 10–18 μm diam were voltage-clamped using the tight-seal whole-cell recording method of Hamill et al. (1981). Electrodes made of borosilicate glass had initial input resistances of 1–4 MΩ when filled with the solutions described later. Typical input resistances in the whole-cell configuration were >2 GΩ. The major component of capacitative currents in response to small voltage pulses usually settled within 200 μs. In most experiments, series resistances before the electronic compensation were 2–6 MΩ, as judged from the settling of the uncompensated capacitative transient currents. Typically, 50% of the series resistance was electronically compensated, resulting in an ~3-mV error for an 800-pA current. Ohmic leak and capacitative currents in the whole-cell records were subtracted by scaling the average current response to 15–20-mV voltage steps. The data presented here were corrected for linear leak and capacitative currents. Unless otherwise noted, holding currents were subtracted from the data. The results are representative of the whole-cell currents from >150 cells.

Single-channel recording. The cell-attached, inside-out, and outside-out configurations of the patch-clamp technique of Hamill et al. (1981) were used to record unitary currents. The initial pipette resistances using the solutions described below were typically 5–15 MΩ. The seal resistances were usually >50 GΩ. Unless otherwise noted, the data presented in this article were obtained using the outside-out configuration of the patch-clamp method. The results are representative of data obtained from >200 patches.

Leak and capacitative currents in the single-channel records were subtracted in the following way. A sweep with no opening was fitted with a sum of several exponentials by eye and the resulting template was subtracted from all the sweeps recorded with the same voltage-clamp parameters. Opening and closing transitions were detected using 50% of the unitary current amplitude at a particular recording voltage as the criterion. Using this criterion, each recording epoch was "idealized." In many patches, more than one type of K^+ channel was observed. When openings of two or more types of K^+ channels overlapped extensively, the data were discarded. Ensemble averages were constructed from the idealized sweeps. The number of channels present in a patch was determined by observing the maximum number of channels open at the same time. In most of the patches, more than one channel was observed. Using the number of channels obtained in this way, the ensemble averages were expressed in probability units.

Current Separation and Solutions

Currents through K^+ channels were isolated from other contaminating currents by using solutions that contained a minimal amount of Na and Cl ions. The external solution usually contained (in millimolar): 145 N-methylglucamine (NMG) aspartate, 2.8 KCl, 2 $MgCl_2$, 10 HEPES (NMG), pH 7.2. The internal solution typically contained (in millimolar): 140 K aspartate, 2 $MgCl_2$, 1 $CaCl_2$, 11 EGTA (10 nM free Ca^{++}), 10 HEPES (NMG), pH 7.2. The internal solution with 1 nM free Ca^{++} was made using 0.11 mM $CaCl_2$ and 11 mM EGTA. The internal solution with 1 μM free Ca^{++} was made using 10 mM $CaCl_2$ and 11 mM EGTA. In some experiments, Cl^- was used in place of aspartate$^-$ in both the internal and external solutions. Other solutions used are described in figure legends. Tetraethylammonium (TEA$^+$) Cl, 4-aminopyridine (4-AP), and quinidine sulfate were obtained from Sigma Chemical Co. (St. Louis, MO). Charybdotoxin (CTX) was a gift from Prof. C. Miller, Brandeis University, Waltham, MA. Experiments were done at room temperature (22–24°C).

RESULTS

Outward Currents Activated by Depolarization

Current-voltage relation. Fig. 1 A shows typical outward currents recorded in PC-12 cells in response to 240-ms depolarizing pulses. Upon depolarization to voltages more positive than 0 mV, the currents activated quickly and did not decline in amplitude noticeably during the pulses. We identified these outward currents as predominantly K^+ currents on the basis of their reversal potentials (see below). The tail currents following the pulses were not well resolved in Fig. 1 A, presumably because the holding voltage (−70 mV) was close to the reversal potential of the K^+ currents (see below). Fig. 1 B shows the peak current–command voltage relation [$I(V_{com})$] of the currents recorded. The outward currents started to activate around −20 mV and increased monotonically in amplitude with greater depolarization. The shape of the $I(V_{com})$ curve and the apparent activation threshold of the outward currents were independent of the current amplitude, which confirms that the voltage error caused by the uncompensated series resistance was negligible. The presence or absence of 2 mM $CaCl_2$ in the external solution did not affect the shape of the peak $I(V_{com})$ in the voltage range of −60 to +40 mV. This observation suggests that, at least in this voltage range, the magnitudes of the K^+ currents through voltage-dependent Ca^{++} channels were negligible (Marty and Neher, 1985). The only marked difference was the shift of $I(V_{com})$ to a more positive direction by 5–10 mV in the presence of 2 mM $CaCl_2$. Even with 2 mM Ca^{++} in the bath, negative slope regions, which are thought to represent activation of Ca^{++}-dependent K^+ currents, were not found in $I(V_{com})$ curves. In most of the cells examined, $I(V_{com})$ curves appeared to saturate at voltages more positive than +100 mV.

Lack of inactivation by prepulses. The amplitudes and time courses of the outward currents were largely independent of the prepulse voltage (−130 to −30 mV). Fig. 1 C shows the effects of prepulses to various voltages on the outward currents recorded at +30 mV. A voltage pulse of either 500 ms (top current records) or 2 s (bottom current records) in duration was given immediately before the test pulse to +30 mV was applied. Prepulses of 500 ms in duration, even to −30 mV, did not visibly decrease the current amplitude (Fig. 1 D). Decreases in the current amplitude were observed only when 500-ms prepulses to the voltages where activation was noticeable (greater than −20 mV) were given. Prepulses lasting 2 s did result in a greater decline in the current amplitude measured at +30 mV. The voltage dependence of the prepulse inactivation (Fig. 1 D) and the voltage dependence of activation (Fig. 1 B) overlapped, leading to a voltage range between −20 and 0 mV, where there was a significant steady state probability of the channels being open. Prepulses to different voltages did not influence the shape of the peak $I(V_{com})$ curves. The effects of the prepulses on the currents recorded at voltages other than +30 mV were similar to those shown in Fig. 1 D.

Time course of activation. Upon depolarization, the outward currents activated, following a sigmoidal time course. The time course of the current activation on a very short time scale recorded at different voltages is shown in
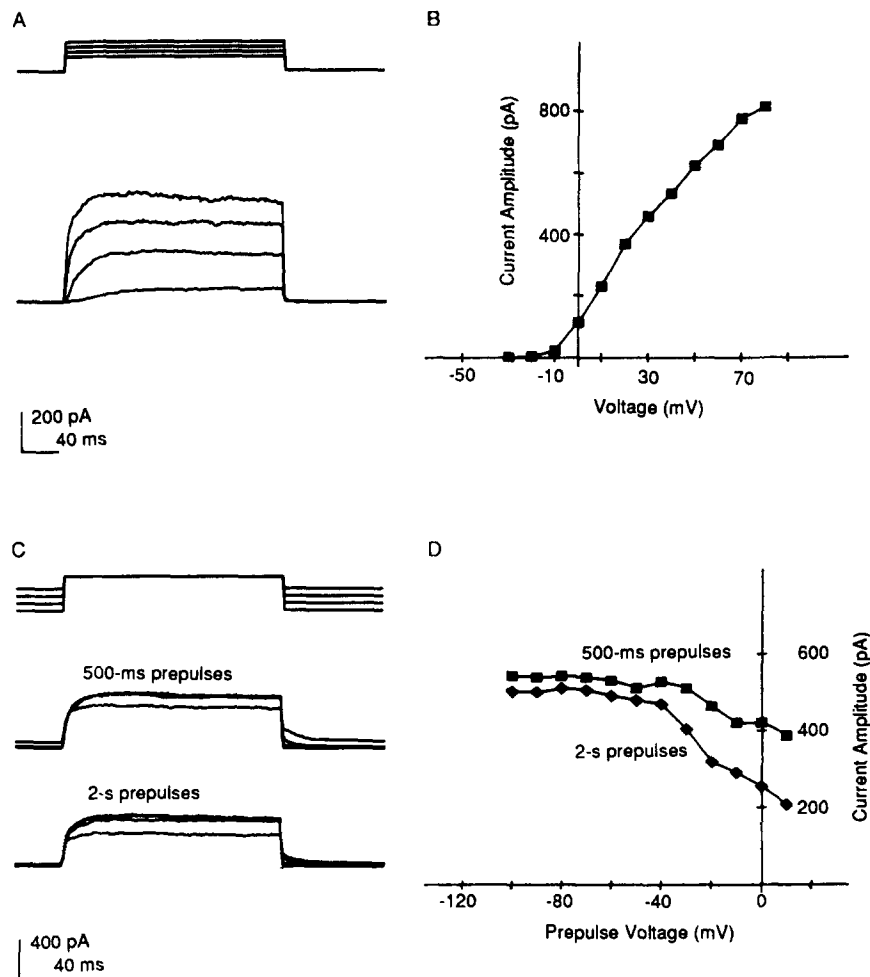
A

B

200 pA
40 ms

C

D

400 pA
40 ms

FIGURE 1. $I(V_{com})$ and $I(V_{pre})$ curves of the whole-cell K⁺ currents. (*A*) Whole-cell K⁺ currents in PC-12 cells elicited in response to voltage pulses from −70 to −10, +10, +30, and +50 mV (from bottom to top). The top shows the voltage pulse protocol. Every fourth point is displayed. Data were filtered at 2 kHz and then digitized at 2.5 kHz. The cell was stimulated every 8 s. The internal solution contained 1 nM free Ca⁺⁺. (*B*) Peak $I(V_{com})$ curve for the K⁺ currents elicited at different voltages from the holding voltage of −70 mV. The peak current amplitudes during 240-ms pulses to the voltages indicated on the abscissa are plotted. (*C*) Effects of prepulses on the K⁺ currents recorded at +40 mV. The top sweeps show the voltage pulse protocol used. Voltage pulses of either 500 ms or 2 s in duration to −100, −70, −40, and −10 mV were applied and then the voltage was changed to +40 mV, where the K⁺ currents were recorded. Every fourth point is displayed. Data were filtered at 2 kHz and digitized at 2.5 kHz. Pulses were applied every 10 s. Same cell as in *A* and *B*. The internal solution contained 1 nM free Ca⁺⁺. (*D*) Peak current–prepulse voltage $[I(V_{pre})]$ curve for the K⁺ currents recorded at +40 mV following prepulses to the voltages indicated on the abscissa. The K⁺ currents were elicited as described in *C*.

Fig. 2A. The currents activated after a delay. For example, there was an ~2-ms delay at +30 mV before the current started to activate markedly (middle sweep). The delay became progressively shorter with greater depolarization. Only a small fraction of the delay was caused by the voltage-clamp settling time (100–200 μs).
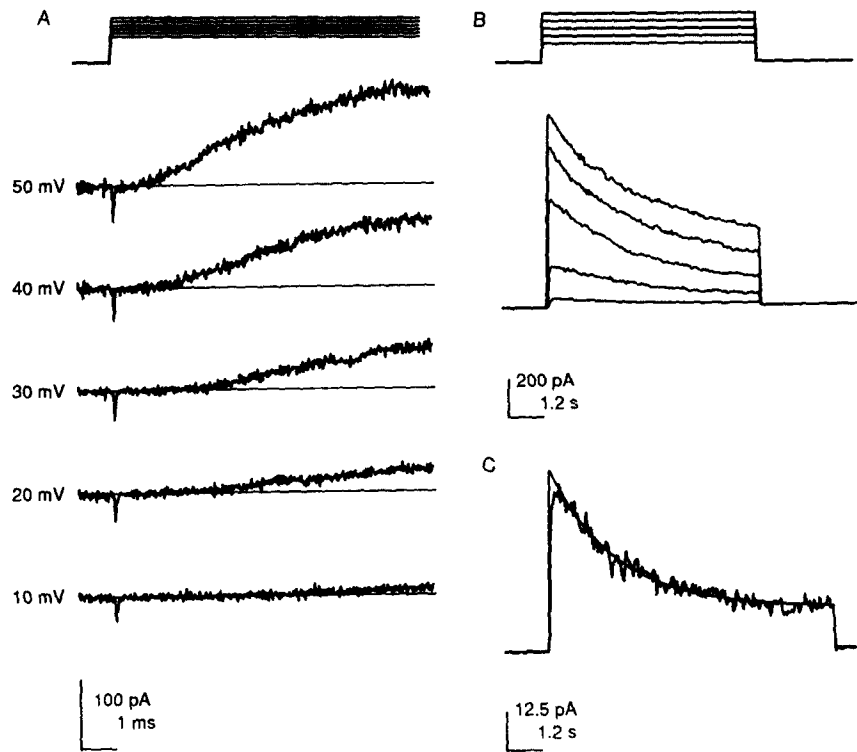

FIGURE 2. Time course of K^+ currents. (A) Sigmoidal activation time course of K^+ currents. The top sweeps show the voltage pulse protocol used and the bottom five sweeps are the K^+ currents recorded at (from bottom to top) 10, 20, 30, 40, and 50 mV. The holding voltage was −70 mV. Data were filtered at 10 kHz and sampled at 50 kHz. Pulses were applied every 5 s. The internal solution contained 10 nM free Ca^{++} and Cl was the major anion. (B) Inactivation of K^+ currents with maintained depolarization. The top sweeps show the voltage pulse protocol used. K^+ currents recorded at (from bottom to top) −20, 0, +20, +40, and +60 mV are shown superimposed. The holding voltage was −70 mV. The pulse duration was 7.2 s. Data were filtered at 1 kHz and sampled at 0.33 kHz. Pulses were applied every 30 s. The internal solution contained 1 nM free Ca^{++}. (C) Inactivation time course of the K^+ currents recorded in response to a 9.6-s pulse from −70 to −20 mV. The time course of the decline of the current was fitted by eye with a single exponential with a time constant of 2.3 s (smooth line). Data were filtered at 500 Hz and sampled at 0.33 kHz.

Prepulses (−120 to −50 mV) for 500 ms did not markedly affect the sigmoidal activation time course of the outward currents. These results suggest that the channels underlying the outward whole-cell current must have at least two closed states before they enter the first open state.

Time course of inactivation. The outward currents declined in amplitude slowly during maintained depolarization. Fig. 2*B* shows outward currents elicited in response to 7.2-s depolarizing pulses. At voltages <0 to +10 mV, the time course of the current decline could be well described by a single exponential plus a steady state, noninactivating component (Fig. 2*C*). The time constants were typically 2–3 s. At more positive voltages (greater than +10 mV), the current decline followed a more complex time course. A sum of at least two exponential components was required. It was not clear whether the current amplitude eventually declined to zero with maintained depolarization. The time course of the decline of the outward current, as measured by the time for the current to decrease to 50% of the peak amplitude, was only slightly dependent on the voltage, being ~2–4 s in the range of −20 to +50 mV. The time course either remained the same in the voltage range or became slightly slower with depolarization. The multiexponential time course of the decline of the outward currents could imply that the underlying K^+ channels have inactivation mechanisms that involve many closed states and/or that PC-12 cells have more than one channel that differ in their inactivation kinetics. The time course of the decline of the K^+ currents recorded at −20 mV could account for the difference in the amount of the prepulse inactivation observed by 500-ms and 2-s prepulses to −20 mV (see Fig. 1*D*). During the 500-ms prepulse, the current elicited by the prepulse declined only slightly. Therefore, most of the channels were still available to open during the test pulse. During the 2-s prepulse, the current inactivated more and the subsequent test pulse elicited a smaller current.

Some variability in the time course of the current decline was observed among the cells examined. We did not systematically examine whether the rate of the decline of the outward current was correlated with other properties of the current. The time course of the current decline often accelerated during the course of an experiment. This acceleration was most noticeable in the initial 3–5 min of achieving the whole-cell configuration, which is consistent with the possibility that the internal dialysis affects the inactivation properties of the underlying channels.

Reversal of tail currents. Tail currents recorded at different voltages following pulses to +30 mV are shown in Fig. 3. At +30 mV, the K^+ channels were fully activated (see below). The tail currents reversed direction, generally in the range of −75 to −80 mV. The calculated equilibrium potential for K^+ was −98 mV. The reversal potential changed as expected for K^+-selective channels when the external K^+ concentration was increased to 140 mM and was not different when Cl^- or aspartate$^-$ solutions were used. The reversal potential of the whole-cell currents was independent of the pulse duration (10–1,000 ms). The tail currents reversed direction around −75 mV after 10- and 1,000-ms pulses to +40 mV. This observation suggests that the inactivation of the K^+ channels, but not accumulation or depletion of K^+, is responsible for the decline in the current amplitude with maintained depolarization up to 1,000 ms.

In the voltage range of −70 to −10 mV, the instantaneous $I(V)$ curve of the outward K^+ currents measured at a fixed time after the voltage change in the tail currents was roughly linear. Inward K^+ tail currents observed at the voltages more negative than −80 mV had a nonlinear instantaneous $I(V)$ curve. The

amplitudes of the inward tail currents were smaller than expected from a linear $I(V)$.

Time course of tail currents. Descriptions of the time course of the tail currents recorded in the voltage range of −120 to −20 mV after 50-ms pulses to +30 mV required a sum of at least two exponential components (Fig. 3). Any
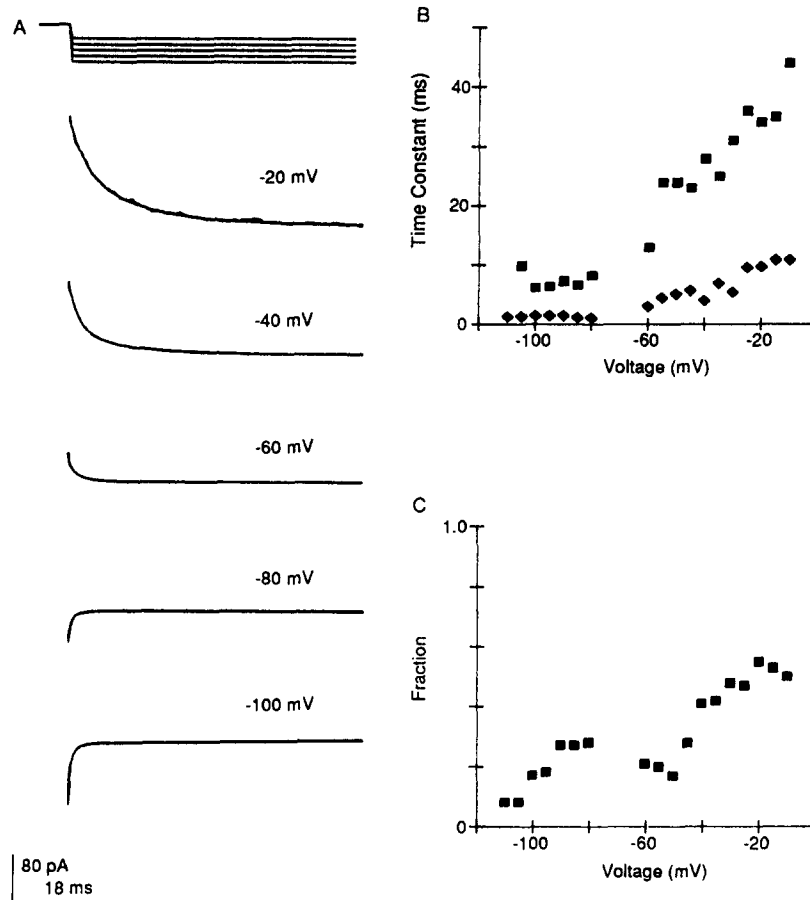

FIGURE 3. Time course of tail currents. (A) Tail currents recorded at −20, −40, −60, −80, and −100 mV. The top traces show the voltage pulse protocol. The cell was depolarized to +30 mV for 50 ms and then repolarized to the voltages indicated. Data were filtered at 1.2 kHz and sampled at 6.7 kHz. The cell was stimulated every 10 s. The time courses of the tail currents were fitted by eye with a sum of two exponential components on normal and expanded time scales. Fitted curves are superimposed on the data traces. The initial two sampled points after the voltage step were not included in the fitting procedure. The recording epochs of 250 ms in duration were fitted. (B) Time constants of the two exponential components used to fit the tail currents. A sum of two exponential components was used to fit the time course of the tail currents recorded at the voltages indicated on the abscissa. The K$^+$ currents were elicited as described in A. (C) Relative amplitude of the longer of the two exponential components used to fit the tail currents.

components of the tail currents faster than 200 μs were not included in the fit. Fig. 3B plots the voltage dependence of the two time constants in the tail currents. The time constants of the two exponential components in the inward tail currents at voltages more negative than −80 mV were voltage independent. The time constants of both the fast and slow components in the outward tail currents increased with depolarization (positive to −50 mV). At every voltage examined, the time constant of the slow component of the tail current was at least three to four times greater than that of the fast component. However, the slow component was more steeply voltage dependent than the fast component, contributing to the overall slower time course of the tail currents in this voltage range. The relative amplitude of the slow component in the tail currents is shown in Fig. 3C. In the voltage range of −100 to −20 mV, the relative amplitudes of the two components were not conspicuously voltage dependent. The long component typically constituted ~20–40% of the tail currents. At more positive voltages (greater than −20 mV), the relative amplitude of the long component increased steeply with further depolarization. At voltages more negative than −100 mV, the relative amplitude of the slow component was very small and the fast component dominated the tail current time course.

Pulse duration and time course of tail currents. The time courses of the tail currents were independent of the pulse durations. Fig. 4 shows the tail currents recorded at −40 mV after pulses to −20 (A) and +20 (C) mV. The durations of the pulses to the two voltages were varied from 5 to 45 ms. Fig. 4B compares the tail currents recorded following 5- and 45-ms pulses to +20 mV. The tail currents following 5-ms pulses were scaled up so that the apparent current amplitudes of the two sweeps were the same at the end of the pulse. The same comparison was made after 10- and 40-ms pulses to −10 mV (Fig. 4D). The tail currents recorded after depolarizing pulses of different durations superimposed well in both cases. These results suggest that the same gating processes were dominant at both 5 and 30 ms after the onset of the depolarizing pulse.

Voltage dependence of activation. The voltage dependence of the fraction of the total conductance activated was measured from the tail currents (Fig. 5). Tail currents were recorded at −40 mV after 100-ms pulses to various voltages. The amplitudes of the tail currents saturated after pulses to voltages more positive than +20 mV. The time courses of the tail currents measured at −40 mV after pulses to different voltages could be fitted by a sum of two exponential components with the same values for the two time constants but with different amplitudes, depending on the pulse voltage. This suggests that the same gating processes were dominant in the voltage range examined.

Fig. 5B plots the tail current amplitudes measured at 5 and 30 ms after the termination of the test pulses (early and late components, respectively) against the test pulse voltage. The voltage dependence of the tail currents at two different times after the pulse termination was fitted by Boltzmann distributions with different parameter values. The fitted curve for the data obtained 30 ms after the pulses (late component) was scaled to match the peak amplitude of the fitted curve for the data obtained 5 ms after the pulses (early component) so that the voltage dependence of the two curves could be compared. The late component of the tail currents consistently activated at 10–15 mV more negative voltages

than the early component. The steepness of the voltage dependence of the curves used to fit the data obtained at different times did not differ in a consistent way. Voltage error caused by the uncompensated series resistance would make the voltage dependence of the early component of the tail currents shift to a more positive voltage since the early component was greater than the late component
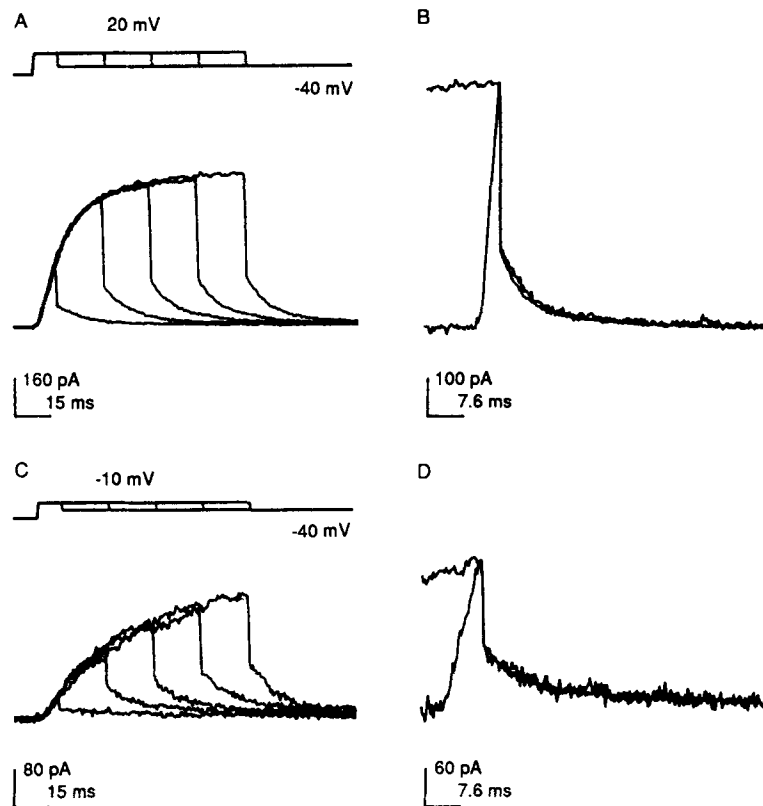

FIGURE 4. Effects of pulse durations on the tail currents. The cell was depolarized to +20 mV in A and −10 mV in C for 5, 15, 25, 35, and 45 ms. Tail currents were recorded at −40 mV following the pulses to +20 mV (A) and −10 mV (B). (B) Tail currents recorded at −40 mV after 5- and 45-ms pulses to +20 mV are compared. The current elicited by the 5-ms pulse was scaled up by a factor of 2.4 so that the apparent current amplitudes at the end of the pulses were identical. (D) Tail currents after 10- and 40-ms pulses to −10 mV are compared as described for B. The current elicited by 10-ms pulses was scaled up 2.2 times so that the apparent current amplitudes of the two sweeps are identical.

in amplitude by a factor of 2.5. To obtain a 10–15-mV shift for the maximal amplitude difference of 80 pA in the data shown, the uncompensated series resistance would have to be >125 MΩ. This much uncompensated series resistance was very unlikely (see Materials and Methods). The fact that the voltage dependence of the early and late components was different could imply that two different types of K^+ channels with different voltage dependences contributed

to the whole-cell currents and/or that the channels had two major gating processes with different voltage dependences.

Transient Currents

In a small number of cells examined (3 out of more than 150 cells), depolarizing pulses elicited very transient K+ currents. K+ currents recorded at different voltages after prepulses to −30 mV (top) and −100 mV (bottom) are shown in Fig. 6. The currents activated quickly and rapidly declined in amplitude to a nonzero steady state level during the 240-ms pulses. The time course of the
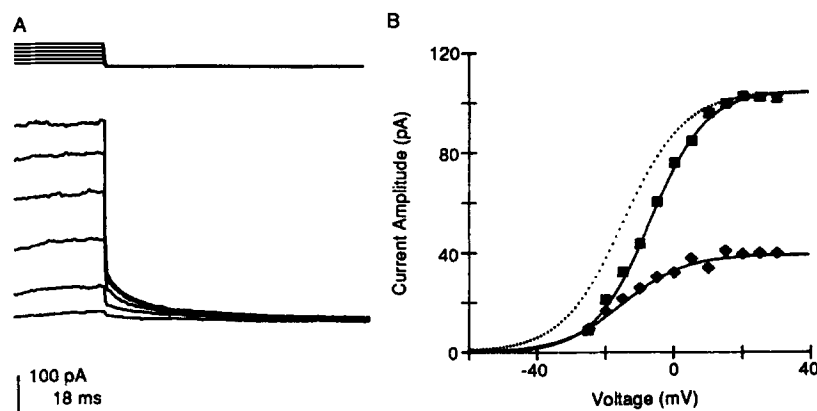

FIGURE 5. Voltage dependence of activation. (A) Tail currents were recorded at −30 mV after 100-ms depolarizing pulses from a holding voltage of −70 mV to −20, 0, +10, +20, and +30 mV (from bottom to top). Data were filtered at 1 kHz and sampled at 2.8 kHz. Pulses were applied every 6 s. (B) Voltage dependence of the amplitudes of the tail currents recorded at 4 ms (squares) and 32 ms (diamonds) after the termination of the pulse. The data were then fitted with Boltzmann functions by eye. The fitted curve for the data obtained after 32 ms was scaled up so that the apparent peak amplitudes of this curve and that for the data obtained 4 ms after the pulse termination are the same (dotted curve). The parameters estimated for the data obtained 4 ms after the pulse are (amplitude, equivalent charge, half-activation voltage) 105 pA, 3.14, and −7 mV and those for the data obtained 32 ms after the pulse termination are 39 pA, 2.82, and −15 mV.

decline in the current amplitude was approximated by a single exponential. The time constant of the decline of the current amplitude was 40–80 ms in the voltage range of +10 to +50 mV, compared with >1 s for the typical K+ currents observed in the majority of the cells examined (see Fig. 2). These transient K+ currents declined in amplitude progressively faster with greater depolarization. The peak $I(V_{com})$ curves of the transient K+ currents (Fig. 6B) were similar to those of the maintained K+ currents described in the previous section. The transient currents were more dependent on the prepulse voltage than the maintained currents (see Fig. 1, C and D). The currents were half-inactivated by the prepulse to about −50 mV. The time course of the decline of the current amplitude was not markedly affected by prepulses to different voltages.

Pharmacology

TEA. External application of 5 mM TEA$^+$ readily blocked the K$^+$ currents in PC-12 cells. Fig. 7A shows K$^+$ currents recorded before (top) and after (bottom) application of 5 mM TEA$^+$. The corresponding peak $I(V_{com})$ curves are shown in Fig. 7B. TEA$^+$ (5 mM) blocked the K$^+$ currents rapidly. At most of the voltages examined, TEA$^+$ did not markedly affect the time course of the K$^+$ currents (Fig. 7C).

4-AP. Bath application of 5 mM 4-AP reduced K$^+$ currents in PC-12 cells. Fig. 8A shows the currents recorded before (top) and after (bottom) application of 5 mM 4-AP. The peak $I(V_{com})$ curves are shown in Fig. 8B. 4-AP (5 mM) usually reduced the peak current amplitudes in a voltage-independent manner.
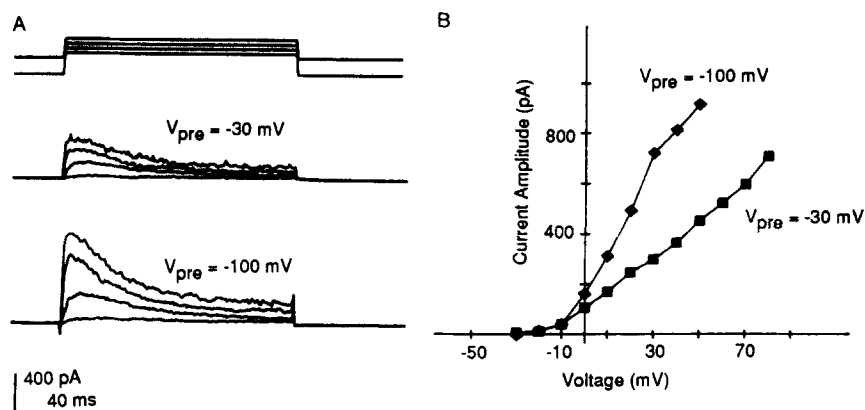

FIGURE 6.   Transient K$^+$ currents. (A) Transient K$^+$ currents observed in a small number of PC-12 cells. The top sweeps show the voltage pulse protocol. K$^+$ currents were recorded at −10, +10, +30, and +50 mV after 500-ms prepulses to −30 and −100 mV. The holding voltage was −50 mV. Data were filtered at 5 kHz and sampled at 10 kHz. Pulses were applied every 5 s. Every 16th data point is displayed. (B) Peak $I(V_{com})$ curves of the K$^+$ currents recorded after 500-ms prepulses to −30 mV (squares) and −100 mV (diamonds).

The fraction of the total outward current blocked by 4-AP remained essentially the same in the voltage range of −10 to +70 mV. Bath application of 4-AP frequently altered the time course of the K$^+$ currents. Fig. 8C compares the current time course before and after application of 5 mM 4-AP. The currents recorded in the presence of 4-AP were scaled up so that the apparent current amplitudes at the end of the pulse were identical in both sweeps. The currents in the presence of 4-AP were often less transient in time course than the control currents. Difference currents, however, were much slower than the transient currents recorded in a small number of PC-12 cells without 4-AP (see Fig. 6). The effectiveness of bath application of 4-AP was variable among the cells examined. The fraction of current blocked by 5 mM 4-AP ranged from 40 to 90%.

CTX. CTX, a basic protein of ∼7 kD derived from a scorpion venom, has been shown to block large Ca^{++}-dependent K$^+$ channels (Miller et al., 1985).

The effects of CTX on K^+ currents in PC-12 cells are shown in Fig. 9. Internal free Ca^{++} concentrations influenced the effects of CTX on the K^+ currents. Fig. 9A shows the currents recorded before (top current sweeps) and after (bottom current sweeps) application of 10 μM CTX using the internal solution containing 10 nM free Ca^{++}. CTX did not noticeably affect the amplitude or time course of the K^+ currents except at voltages more positive than +80 mV, where it
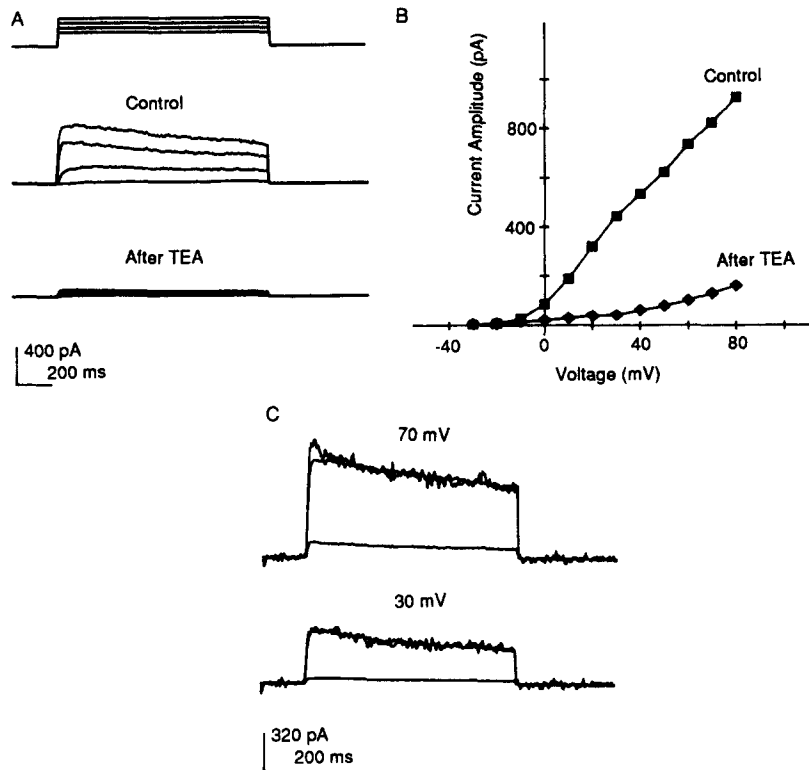

FIGURE 7.   Effects of TEA^+ on K^+ currents. (A) K^+ currents recorded at −10, +10, +30, and +50 mV before and after addition of 5 mM TEA-Cl to the bath. The holding voltage was −70 mV. Data were filtered at 1.5 kHz and sampled at 0.5 kHz. Every fourth data point is displayed. Pulses were applied every 5 s. (B) Peak $I(V_{com})$ curves of K^+ currents before (squares) and after (diamonds) addition of 5 mM TEA^+ to the bath. (C) Comparison of the time course of the K^+ currents recorded at +70 mV (top) and at +30 mV (bottom) before and after 5 mM TEA^+. The holding voltage was −70 mV. For each voltage, three sweeps are shown: (a) K^+ current before TEA^+, (b) K^+ current after TEA^+ (smallest sweeps), and (c) K^+ current recorded after TEA^+, scaled up so that the apparent current amplitude at the end of the pulse was the same as that of the current before TEA^+ application (noisy sweeps).

reduced the current amplitudes slightly (Fig. 9A). CTX blocked K^+ currents more effectively when the internal solution contained 1 μM free Ca^{++} (Fig. 9D). With 1 μM free Ca^{++} in the internal solution, the activation time course of the K^+ currents was frequently faster than that observed with 1 or 10 nM free Ca^{++}. CTX reduced the current amplitudes in a voltage-dependent manner, being

more effective at voltages more positive than +20 mV. No other marked changes in the properties of the whole-cell K^+ currents were observed when the internal solution with 1 μM Ca^{++} was used in place of that with 1 or 10 nM Ca^{++}.

Single-channel recordings show that PC-12 cells contain many large Ca^{++}-dependent K^+ channels that are readily blocked by CTX (see below). Studies of
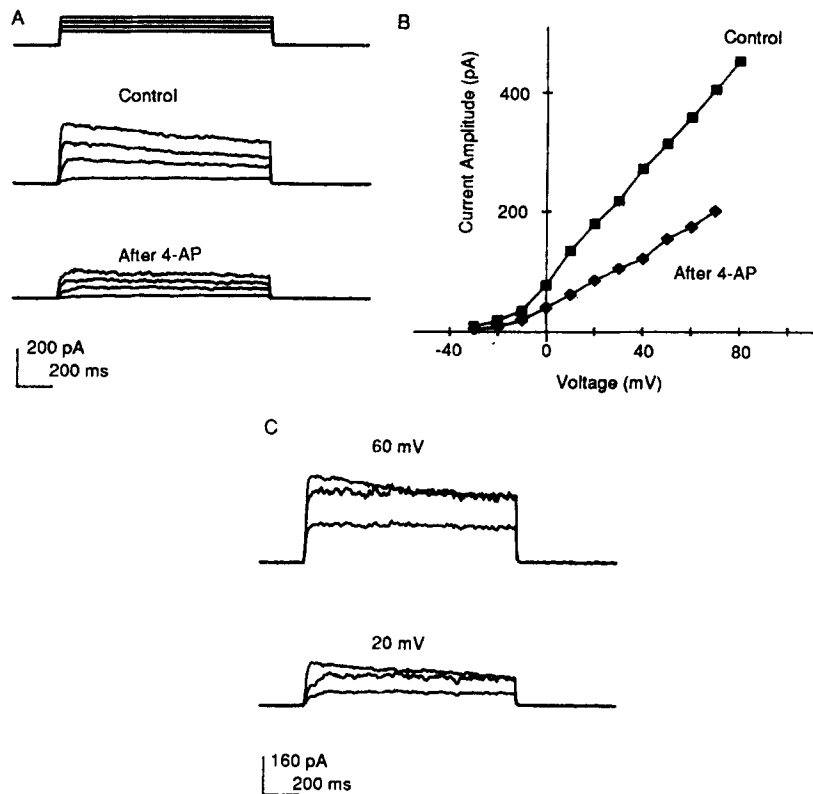

FIGURE 8.   Effects of 4-AP on K^+ currents. (A) K^+ currents recorded at −10, +10, +30, and +50 mV before and after addition of 5 mM 4-AP to bath. The holding voltage was −70 mV. Data were filtered at 1 kHz and sampled at 0.5 kHz. Every fourth data point is displayed. Pulses were applied every 5 s. (B) Peak $I(V_{com})$ curves of K^+ currents before (squares) and after (diamonds) 5 mM 4-AP. (C) Comparison of the time course of the K^+ currents recorded at +60 mV (top) and at +20 mV (bottom) before and after 5 mM 4-AP. The holding voltage was −70 mV. For each voltage, three sweeps are shown: (a) K^+ current before 4-AP, (b) K^+ current after 4-AP (smallest sweeps), and (c) K^+ current recorded after 4-AP, scaled so that the apparent current amplitude at the end of the pulse was the same as that of the current before 4-AP application (noisy sweeps).

the voltage dependence of gating of large Ca^{++}-dependent K^+ channels showed that, in the presence of 10 nM free Ca^{++}, the probability of these channels being open is negligible. In the presence of 1 μM Ca^{++}, the probability is much greater at +40 mV (e.g., Barrett et al., 1982). Differential effects of CTX on the K^+ currents, depending on the internal free Ca^{++} concentration, were consistent

with these results of Ca⁺⁺ dependence of large Ca⁺⁺-dependent K⁺ channels. These effects of CTX suggest that Ca⁺⁺-dependent K⁺ channels contributed little to the whole-cell currents presented so far in this article using 1 or 10 nM free Ca⁺⁺ in the internal solution.
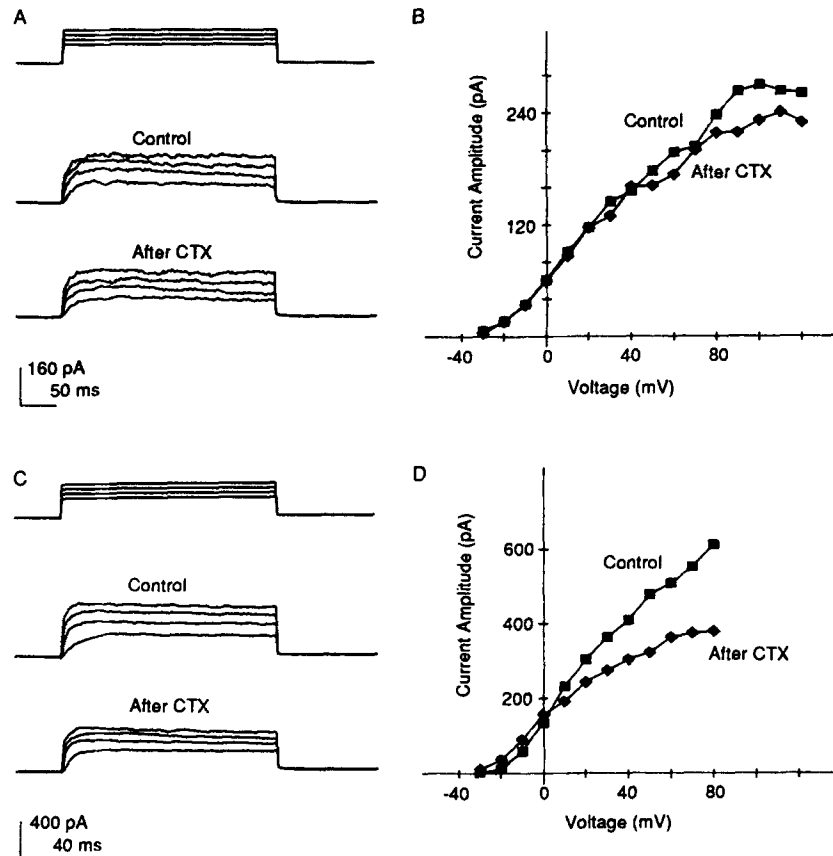

FIGURE 9.   Effects of CTX on K⁺ currents. (*A*) K⁺ currents recorded at +10, +30, +50, and +70 mV using the internal solution containing 10 nM free Ca⁺⁺ before and after application of 10 μM CTX to bath. The pulse duration was 300 ms. The holding voltage was −70 mV. The top sweeps show the voltage pulse protocol. Data were filtered at 2 kHz and sampled at 2 kHz. Pulses were applied every 5 s. Every fourth point is displayed. Cl was the major anion. (*B*) Peak *I*(*V*com) curves of the K⁺ currents recorded before (squares) and after (diamonds) application of 10 μM CTX to the bath using the internal solution with 10 nM free Ca⁺⁺. (*C*) K⁺ currents recorded at +10, +30, +50, and +70 mV using the internal solution containing 1 μM free Ca⁺⁺ before and after application of 20 μM CTX to the bath. The holding voltage was −70 mV. The top sweeps show the voltage pulse protocol. The pulse duration was 240 ms. Note that the pulse duration is shorter than that shown in *A*. Data were filtered at 1 kHz and sampled at 2.5 kHz. Every fourth point is displayed. Pulses were applied every 8 s. (*D*) Peak *I*(*V*com) curves of the K⁺ currents recorded before (squares) and after (diamonds) application of 20 μM CTX to the bath using the internal solution with 1 μM free Ca⁺⁺.

Quinidine. Quinidine (500 μM) rapidly and completely blocked the whole-cell K^+ currents. Its effects were also very readily reversible. Block of the K^+ currents by 500 μM quinidine was much more complete, faster, and more reversible than that by 5 mM TEA$^+$ or 5 mM 4-AP. Quinidine blocks various K^+ channels (see below) but does not affect voltage-dependent Ca^{++} channels (Hoshi et al., 1984). This also suggests that outward K^+ currents through the voltage-dependent Ca^{++} channels, as seen in adrenal chromaffin cells (Marty and Neher, 1985), were negligible in PC-12 cells.

Properties of Single K^+ Channels in PC-12 Cells

In response to depolarizing pulses, openings of at least five types of K^+ channels were observed. These different classes of K^+ channels could be distinguished on the basis of their unitary current amplitudes, open-channel current-voltage [$i(V)$] curves, and other characteristics. One of the five types was the large Ca^{++}-dependent K^+ channel also described in other preparations (for review see Marty, 1983b; Latorre et al., 1984). We focus on the four types of smaller K^+ channels and do not include extensive descriptions of large Ca^{++}-dependent K^+ channels. Fig. 10 shows openings of the four types of voltage-dependent K^+ channels elicited by depolarizing voltage steps in four separate patches, each of which contained channels from a single class. We call the channels shown in Fig. 10 the K_W (A), K_Z (B), K_Y (C), and K_X (D) channels. Their typical chord conductance values in the range of 0 to +40 mV using our standard solutions were ~18, 12, 7, and 7 pS. K_Y and K_X channels had very similar chord conductance values in this voltage range.

Among the four types of the voltage-dependent K^+ channels mentioned, the K_Z channels were most frequently observed in PC-12 cells. K_Y and K_X channels were also observed frequently. However, their small unitary current amplitudes at most voltages made them difficult to study. The K_W channels were least frequently observed. In addition to the four types of channels mentioned above, other outward unitary currents were also observed occasionally. These small unitary currents must have flowed through K^+ channels because they were observed even when the majority of Cl^- was replaced with aspartate$^-$, and the unitary current amplitudes changed with voltage as expected for K^+ channels when the normal saline solutions were used. However, these channels were observed too infrequently and were too small in the unitary current amplitude to study. The four types of K^+ channels shown in Fig. 10 and large Ca^{++}-dependent K^+ channels accounted for the majority of K^+ channels present in PC-12 cells that we could study.

For each type of channel, ensemble averages are shown below the individual sweeps. The K_W channels (Fig. 10A) showed the most transient behavior; the probability of the channel being open increased and then declined quickly during depolarizing pulses. K_Y and K_X channels (Fig. 10, C and D) showed the least transient behavior; the probability of the channel being open did not decline noticeably during depolarization. The K_Z channel (Fig. 10B) showed intermediate properties; the probability of the channel being open increased quickly on depolarization and then declined more slowly than that of the K_W channels but more rapidly than that of either K_Y or K_X channels.

PC-12 cells had a very high density of these voltage-dependent K⁺ channels. Even when seals were made with electrodes with initial input resistances >20–25 MΩ, the patches almost always contained more than one channel. Although we did not observe all four types of K⁺ channels in a single patch, at least three
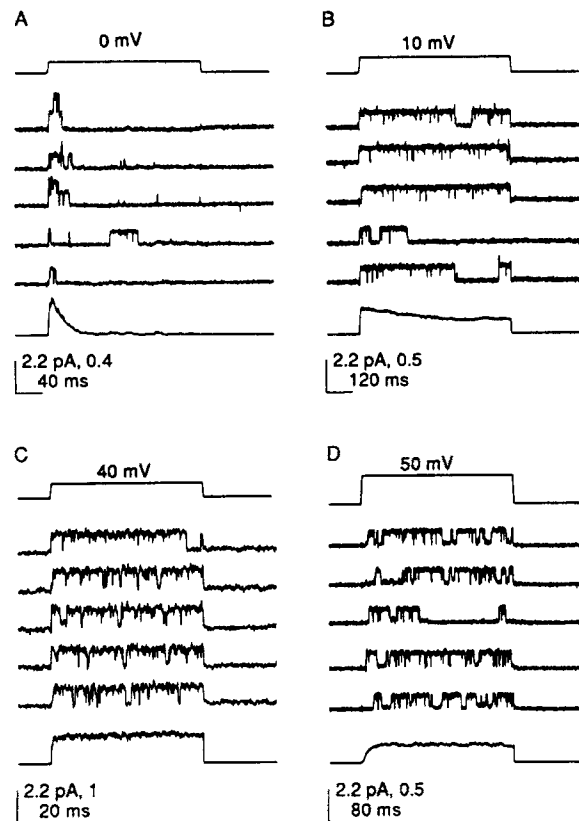

FIGURE 10.   Representative openings of single K⁺ channels. Representative openings of the four types of voltage-dependent K⁺ channels in PC-12 cells. The figure shows the records from the K_W (*A*), K_Z (*B*), K_Y (*C*), and K_X (*D*) channels. In each section, the top shows the voltage pulse protocol used to elicit the openings. The bottom sweeps are the ensemble averages, showing the time course of the probability of the channel being open. Note that amplitude and time scale bars are different. (*A*) The patch was depolarized to 0 from −70 mV. Data were filtered at 1 kHz and sampled at 10 kHz. (*B*) The patch was depolarized to 10 from −90 mV. Data were filtered at 1 kHz and sampled at 3.3 kHz. (*C*) The patch was depolarized to 40 from −50 mV. Data were filtered at 1 kHz and sampled at 10 kHz. (*D*) The patch was depolarized to +50 mV after 1-s prepulses to −130 mV. Data were filtered at 1 kHz and sampled at 5 kHz.

of the four types were often observed (see Fig. 12). We did not notice any marked differences in the frequency with which these four different types of channels were observed in cells plated on coverslips for a different number of days. We did not systematically test whether these four different types of K⁺ channels were localized to different regions of the cells.

Open-Channel i(V) Curves

Fig. 11 compares the open-channel $i(V)$ curves of the four types of K^+ channels obtained using voltage ramps. The internal solution did not contain any added Na^+ to avoid very fast block of K^+ channels by Na ions (Marty, 1983a; Yellen, 1984). For each record, a straight line was fitted to the linear portion of the open-channel $i(V)$ curves. In the excised configurations using the Na^+-free solutions described in Materials and Methods, the slope conductances of the linear portion of the open-channel $i(V)$ curves of the K_W, K_Z, K_Y, and K_X channels were 15–19, 10–14, 5–9, and 5–9 pS, respectively.

None of the four types of K^+ channels had linear $i(V)$ curves in the entire voltage range of −70 to +100 mV. The K_W, K_Z, and K_X channels had sublinear $i(V)$ curves; the current amplitudes saturated at voltages more positive than +60 to +80 mV. K_Y channels had a supralinear $i(V)$ curve. The difference in the
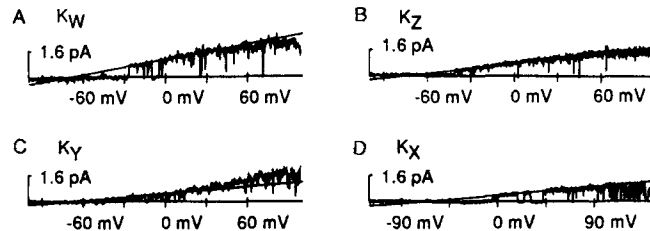

FIGURE 11.   Open-channel $i(V)$ curves. Open-channel $i(V)$ curves of the K_W (A), K_Z (B), K_Y (C) and K_X (D) channels are shown. The open-channel $i(V)$ curves were obtained by using ramp voltage stimuli. In A, the data were filtered at 1 kHz and sampled at 10 kHz (1.7 mV/ms). In B, the data were filtered at 1 kHz and sampled at 2.5 kHz (0.4 mV/ms). In C, the data were filtered at 2 kHz and sampled at 10 kHz (1.7 mV/ms). In D, the data were filtered at 2 kHz and sampled at 10 kHz (1.1 mV/ms). Leak currents have been subtracted from the records. Straight lines represent 17 (A), 12 (B), 8 (C), and 7 (D) pS.

open-channel $i(V)$ property between the K_Y and K_X channels was one of the characteristics that distinguished these two types of channels, which had similar unitary current amplitudes at some voltages. Essentially the same open-channel $i(V)$ curves were obtained using the amplitudes of the openings elicited by step voltage pulses. Extrapolated reversal potentials of the four types of channels were similar to the K^+ equilibrium potentials. When the external K^+ concentration was increased to 140 mM so that the equilibrium potential of K^+ was ~0 mV, the open-channel $i(V)$ curves of these channels reversed in direction around 0 mV. Thus, these four types of channels are in fact K^+ channels. These K^+ channels were also observed when most of the Cl ions were replaced with aspartate⁻.

Pharmacology

The sensitivities of the four types of voltage-dependent K^+ channels to external applications of TEA^+, 4-AP, CTX, quinidine, and apamin were examined.

TEA. Fig. 12A shows the effects of external application of TEA^+ (5 mM) on a patch containing K_W, K_Y, or K_X, and large Ca^{++}-dependent K^+ channels.
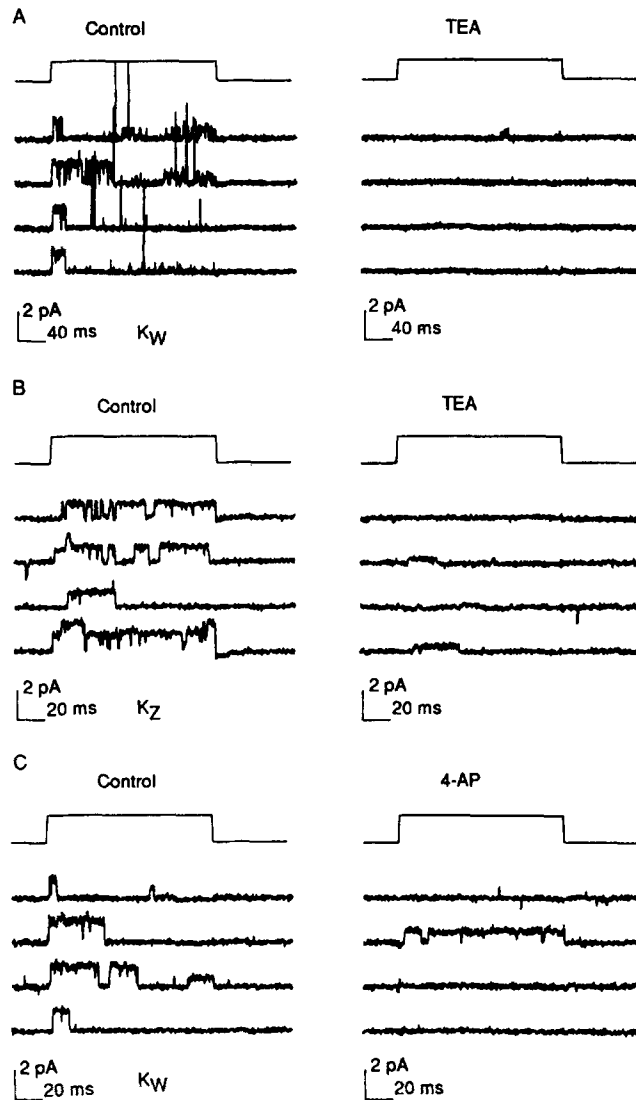
FIGURE 12.   Pharmacology of K^+ channels. (A) Effects of bath application of 5 mM TEA-Cl to a patch containing large Ca^{++}-dependent K^+ channels, a K_Z channel, and a K_X or K_Y channel. It is not clear which of the K_X or K_Y channels was present. The patch was depolarized to $+10$ mV for 240 ms after 500-ms prepulses to -100 mV. Brief spiky events are the openings of the large Ca^{++}-dependent K^+ channels. Data were filtered at 1 kHz and sampled at 10 kHz. The major anion was Cl and the internal solution contained 10 nM Ca^{++}. (B) Effects of bath application of 5 mM TEA-Cl to a patch containing K_Z channels. The patch was depolarized to $+30$ from -70 mV after 250-ms prepulses to -120 mV. Data were filtered at 1 kHz and sampled at 10 kHz. The major anion was Cl and the internal solution contained 10 nM Ca^{++}. (C) Effects of bath application of 1 mM 4-AP to a patch containing K_W channels. The patch was depolarized to $+20$ from -60 mV after 250-ms prepulses to -140 mV. Data were filtered at 1 kHz and sampled at 10 kHz. The major anion was Cl and the internal solution contained 10 nM Ca^{++}.

TEA^+ (5 mM) blocked all three types of the channels present in this patch, although the smallest channels (K_Y or K_X) appeared slightly more resistant to TEA^+ than the other two. The K_Z channel was also readily blocked by 5 mM TEA^+ (Fig. 12B).

4-AP. Fig. 12C shows the effects of application of 1 mM 4-AP to a patch containing K_W channels. 4-AP drastically reduced the frequency of openings. The effects of 4-AP on the K_Z channel were variable among the patches examined. 4-AP appeared to reduce the frequency of openings of the K_W and K_Z channels without markedly affecting the single-channel current amplitude. In the presence of 4-AP in the bath, openings of some channels that we could not readily identify were also observed.

CTX. CTX (20 μM) blocked the large Ca^{++}-dependent K^+ channels. It did not, however, block K_Z channels. We did not test whether CTX blocks K_W, K_Y, or K_X channels.

Quinidine. Quinidine (100 μM and 1 mM) blocked all the types of K^+ channels tested: K_Z, K_Y, K_X, and large Ca^{++}-dependent K^+ channels. We did not test the effects of quinidine on the K_W channels. In the presence of quinidine, the K_Z, K_Y, and K_X channels described in Fig. 10 did not open at all. Large Ca^{++}-dependent K^+ channels opened only at voltages more positive than +120 mV in the presence of quinidine. Openings of the large Ca^{++}-dependent K^+ channels in the presence of quinidine were reduced in unitary amplitude and the open durations were extremely short. The burst durations of large Ca^{++}-dependent K^+ channels, however, appeared greater in the presence of quinidine. The blocking effects of quinidine were rapidly reversible.

Apamin. Apamin (0.1 μM) did not affect large Ca^{++}-dependent K^+ channels or K_Z channels. We did not test the effects of apamin on other types of K^+ channels.

Ca^{++} dependence. All four types of voltage-dependent K^+ channels shown in Fig. 10 were observed using an internal solution containing 1 nM or 10 nM free Ca^{++}. When the internal solution containing 1 μM free Ca^{++} was used, there were no marked changes in the frequency with which any of the K^+ channels, except for the large Ca^{++}-dependent K^+ channels, were observed. Thus, these K^+ channels did not directly require a high concentration (micromolar range) of internal free Ca^{++} to open, although Ca^{++} may regulate some properties of these channels.

Voltage Dependence

K_Z channels. Some representative openings of the K_Z channels recorded at different voltages in response to 336-ms pulses are shown in Fig. 13A. At low voltages (−50 to −45 mV), the channel did not open immediately after the depolarization. With greater depolarization, the channels opened rapidly on depolarization and the apparent burst durations were greater than those at more negative voltages. We occasionally observed openings in some patches of a channel very similar to those of the K_Z channel but with ~50% of the unitary current amplitude. It is not clear whether these openings represent a substate of the K_Z channel or a different class of channel with kinetics very similar to that of K_Z channels.
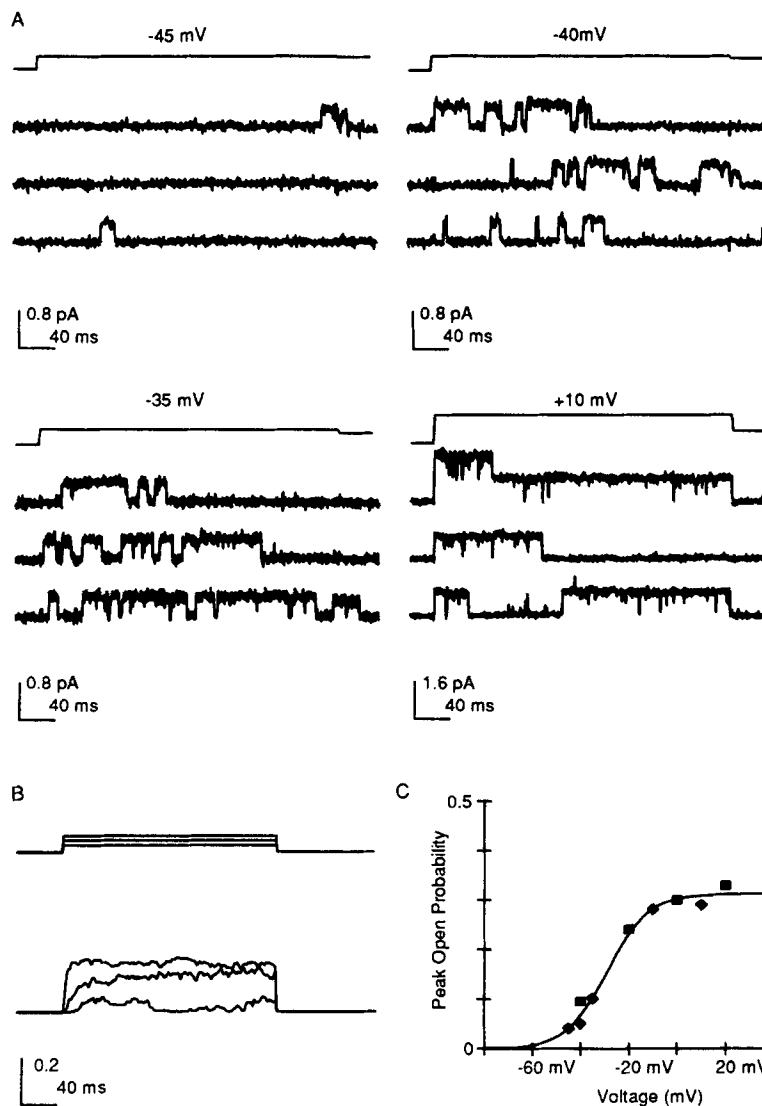
FIGURE 13. Voltage-dependent activation of K_Z channels. (A) Openings of the K_Z channels recorded at −45, −40, −35, and +10 mV. The patch was depolarized from a holding voltage of −90 mV to the voltages indicated for 336 ms and then repolarized to −50 mV. At each voltage, three representative but not consecutive sweeps are shown. Data were filtered at 500, 500, 700, and 1,000 Hz at −45, −40, −35, and +10 mV, and sampled at 10 kHz. (B) Ensemble averages of the openings of the K_Z channels recorded at −40, −20, and 0 mV (from bottom to top). The patch was depolarized from a holding voltage of −70 mV to these voltages. Ensemble averages were digitally filtered at 200 Hz. (C) Voltage dependence of the probability of the K_Z channel being open. Data obtained from two different patches are shown with different symbols. The peak probabilities of the channel being open were measured from the ensemble averages and are plotted against the test voltages. The data were fitted with a Boltzmann function with an equivalent charge of ~3 and a half-maximum voltage of −28 mV.

Ensemble averages showing the time courses of the probabilities of the channel being open are shown in Fig. 13B. The peak probability of the channel being open is plotted against voltage in Fig. 13C. The channel started to open around −40 to −30 mV and the probability reached the plateau level at about +10 to +20 mV. The data shown in Fig. 13C were fitted by a Boltzmann distribution with an equivalent charge movement of ~3 and a half-activation voltage of about −30 mV.

Fig. 14A shows the ensemble average current of the K_Z channel at +20 mV when the pulse duration was increased to 2.4 s. The probability of the channel being open declined to 50% of the maximum value in ~500 ms in the data shown. The time course of the decline of the open probability varied greatly among the patches examined, ranging from 100 to 600 ms. This was the most variable property of the K_Z channels. The averages shown in Fig. 13B showed less inactivation than most others examined. It appeared that the variability in the number of bursts observed in each depolarizing epoch might account for the variability in the inactivation time course. The voltage dependence of the peak probability of the channel being open, the voltage dependence of the inactivation by prepulses (see below), the mean open times, and the first latencies (see Hoshi and Aldrich, 1988) did not markedly vary depending on the time course of the decline of the peak probability. Within a given patch, the time course of the decline of the probability of the K_Z channel being open accelerated with greater depolarization in the range of −40 to +10 mV.

Fig. 14B shows the inactivation properties of the K_Z channel recorded at 0 mV on a slower time scale. The patch was depolarized from a holding voltage of −80 mV to 0 mV immediately before the recording began. The four traces are a continuous recording. On depolarization, at least five channels opened and gradually all the channels closed. With time, however, some channels did reopen. After the last opening, shown in Fig. 14B, no more openings could be observed until the patch was repolarized to −80 mV and then back to 0 mV again (>1 min). The steady state probability of the K_Z channel being open at 0 mV was negligible. The time course of the decline of the probability of the channel being open shown in Fig. 14B appeared to follow a sum of two exponential components, which suggests that at least two closed states are involved in the inactivation process. Since the steady state probability of the channel being open was about nil, one of the two states must be an absorbing state at this voltage.

Prepulse voltages affected the probability of the K_Z channel being open. Fig. 15A shows the ensemble averages of K_Z channel openings recorded at +20 mV after 500-ms prepulses to −130, −70, and −30 mV. Prepulses to more positive voltages decreased the peak probability of the channel being open. Fig. 6B plots the peak probability that the channel is open against the prepulse voltage. In most of the patches, the relationship between the open probability and the prepulse voltage did not appear to follow a simple Boltzmann distribution. During the course of an experiment, the dependence of the probability of the K_Z channel being open on the prepulse voltage often changed. With time, more negative prepulses were required to elicit the openings.

The free Ca^{++} concentration on the cytoplasmic side of the membrane affected the dependence of the peak probability of the channel being open on the prepulse
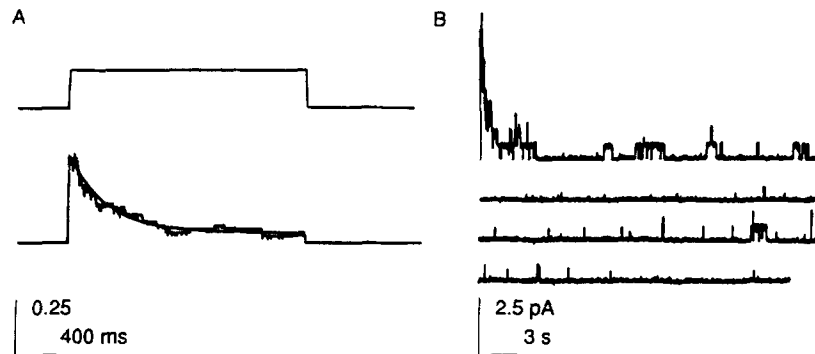
A

B

| 0.25
| 400 ms

| 2.5 pA
| 3 s

FIGURE 14. Inactivation of K_Z channels with maintained depolarization. (A) Ensemble average of the openings of the K_Z channels recorded in response to 2.4-s pulses to +20 mV after 512-ms prepulses to −120 mV. The holding voltage was −70 mV. Pulses were applied every 10 s. The data were filtered at 1 kHz and sampled at 1 kHz. The smooth line is an exponential fit to the declining phase of the ensemble average (by eye). The time constant was 570 ms. (B) Inactivation of the K_Z channel with maintained depolarization. The patch was depolarized from a holding voltage of −80 to 0 mV immediately before the recording began. Data were filtered at 1 kHz and sampled at 5 kHz and then digitally filtered at 50 Hz. The traces form a continuous record 1.7 min long. Brief spiky events of various amplitudes are the unresolved openings of large Ca^{++}-dependent K^+ channels.

voltage. During experiments using the inside-out configuration, the dependence of the peak probability of the channel being open on the prepulse voltage was measured with the solutions containing 1 μM and 10 nM free Ca^{++}. The probability of the channel being open was measured after 240-ms prepulses to −100, −70 and −40 mV. With the prepulses to −100 and −40 mV, free Ca^{++} did not affect the open probability. With the prepulses to −70 mV, the open

A

B

| 0.2
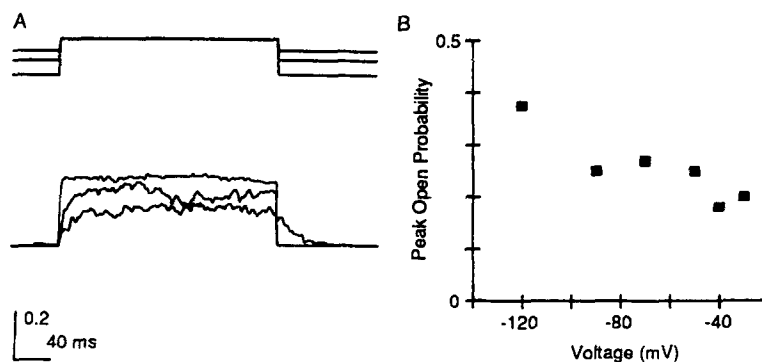| 40 ms

Peak Open Probability

Voltage (mV)

FIGURE 15. Effects of prepulses on the K_Z channel. (A) Ensemble averages of the openings recorded at +20 mV after 500-ms prepulses to −120, −70, and −30 mV (from bottom to top). Pulses were applied every 5 s. Ensemble averages were digitally filtered at 200 Hz. (B) Dependence of the peak probability of the channel being open on the prepulse voltage. Peak probabilities were measured from the ensemble averages constructed as described in A.

probability in the presence of 1 μM Ca^{++} was 50% of that in the presence of 1 nM Ca^{++}. This shift could be explained by the more effective screening of the negative surface charges on the membrane by Ca^{++} when the concentration was 1 μM.

K_Y channels. Ensemble averages of the openings of a K_Y channel recorded at two different voltages after prepulses to -50 and -100 mV are shown in Fig.
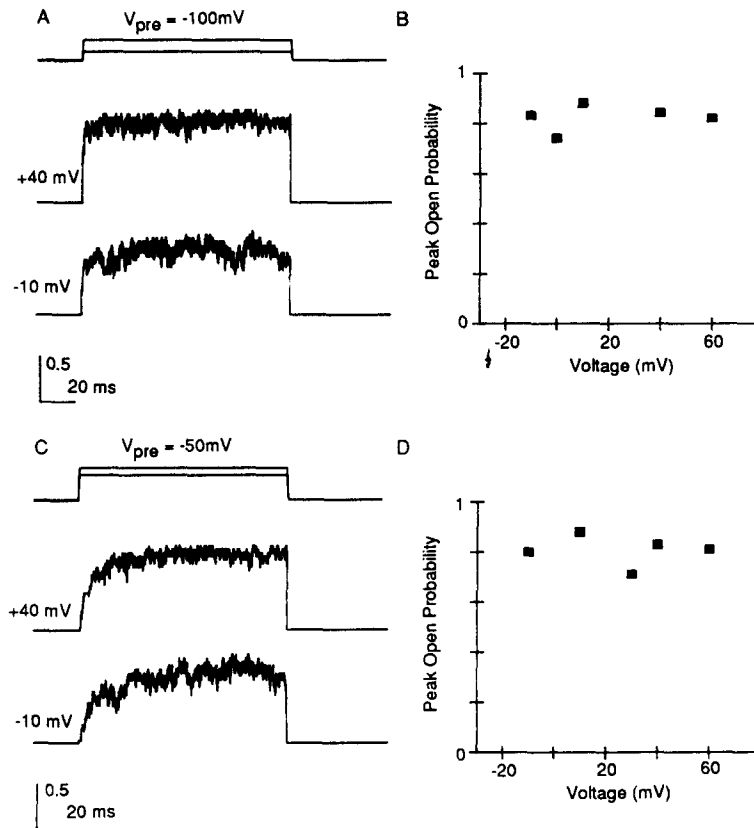

FIGURE 16. Voltage dependence of the K_Y channel. (A and C) Time courses of the probabilities of the channel being open. Ensemble averages of the channel openings recorded at -10 and $+10$ mV without prepulses (A) and after prepulses to -100 mV for 250 ms (C) are shown. The holding voltage was -50 mV. Data were filtered at 1 kHz and sampled at 10 kHz. (B and D) Peak probability of the channel being open without hyperpolarizing prepulses (B) and with prepulses to -100 mV for 250 ms (D). The holding voltage was -50 mV.

16, A and C. The time course of the probability of the channel being open did not vary markedly in the voltage range of -10 to $+60$ mV. The probabilities of the channel being open at various test voltages following prepulses to -50 mV are shown in Fig. 16B and those obtained using the prepulses to -100 mV are shown in Fig. 16D. Regardless of the prepulse voltage, the peak open probability was roughly unity at test voltages more positive than -10 mV. Most of the

voltage-dependent gating that changed the overall probability of the channel being open must have occurred at more negative voltages, where the unitary current amplitudes of the channel were too small to study.

The peak probability of the K_Y channel being open was not markedly affected by depolarizing prepulses. The prepulses, however, did influence the activation
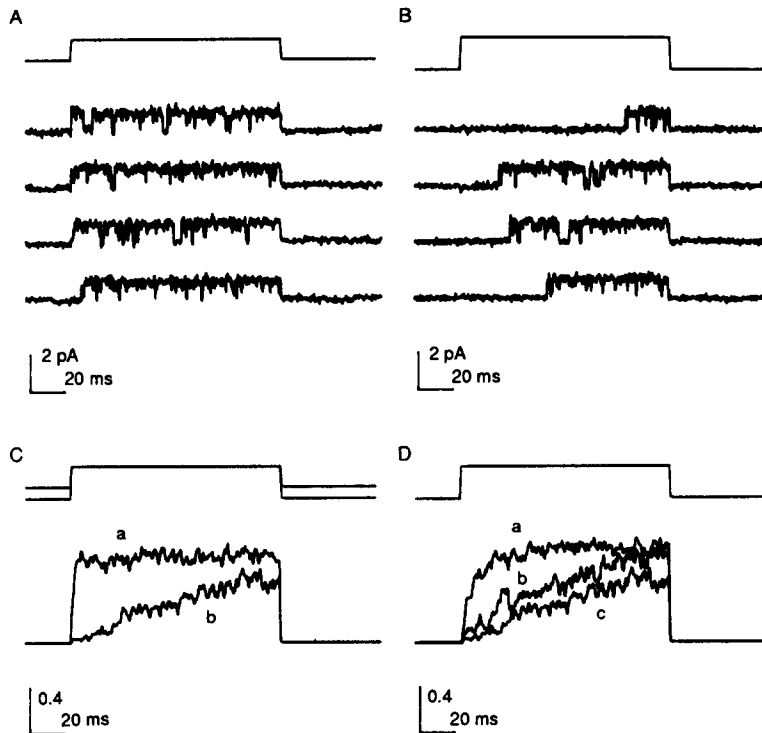

FIGURE 17.   Effects of prepulses on the ensemble averages of the K_Y channel. (A and B) Representative openings of a K_Y channel recorded at +40 mV with 2-s prepulses to −100 mV (B) and without the prepulses (A). The holding voltage was −50 mV. The patch was directly depolarized to +40 mV from the holding voltage of −50 mV in A and after 2-s prepulses to −100 mV (B). Pulses were applied every 5 s. Data were filtered at 1 kHz and sampled at 10 kHz. (C) Ensemble averages of the openings of a K_Y channel recorded at +40 mV with 2-s prepulses to −100 mV (b) and without the prepulses (a). The holding voltage was −50 mV. Openings were elicited as described for A and B. (D) Ensemble averages of the openings of a K_Y channel recorded at +40 mV after prepulses to −100 mV for 250, 1,000, and 2,000 ms. The patch was first hyperpolarized to −100 mV from a holding voltage of −50 mV for 250 (a), 1,000 (b), and 2,000 (c) ms, and then depolarized to +40 mV, where the openings were recorded. Pulses were applied every 5 s. Data were filtered at 1 kHz and sampled at 10 kHz.

time course of the K_Y channel. Hyperpolarizing prepulses slowed the activation time course of the K_Y channel, whereas depolarizing prepulses accelerated the time course. Fig. 17, A–C, compares the openings and the ensemble averages recorded at +40 mV with and without hyperpolarizing prepulses to −100 mV. The peak probability levels reached by the average currents elicited after

prepulses to the two different voltages were approximately the same. However, the time course of the activation of the ensemble average following prepulses to -100 mV was clearly slower than that following prepulses to -50 mV. The prepulses did not simply lengthen the initial delay component in the sigmoidal activation time course but also slowed the major component of the activation (cf. Cole and Moore, 1960). In the data shown in Fig. 17, A–C, the activation rates, as measured by the time to reach 50% of the peak probability of the channel being open with and without the hyperpolarizing prepulses, were 1 and 50 ms, respectively.

The duration of the prepulses also affected the activation time course of the K_Y channel. Fig. 17D shows three ensemble averages of the K_Y channel openings recorded at $+40$ mV following prepulses to -100 mV. Ensemble averages a, b,
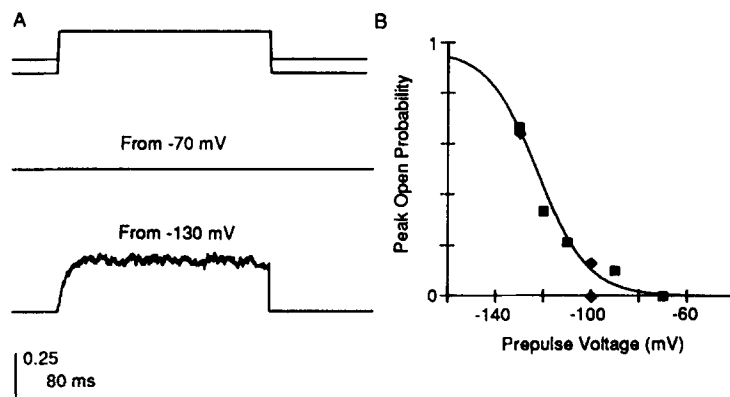

FIGURE 18. Ensemble averages of the K_X channel. (A) Ensemble averages of the openings of the K_X channel recorded at $+50$ mV with prepulses to -130 mV and without prepulses. The holding voltage was -70 mV. Data were filtered at 5 kHz and sampled at 5 kHz. Pulses were applied every 5 s. (B) Dependence of peak probability of the channel being open on the prepulse voltage. The patch was depolarized to $+50$ mV after prepulses to the voltages indicated on the horizontal axis for 1,000 ms (squares) or for 240 ms (diamonds). Data were fitted with a Boltzmann function with an equivalent charge movement of 2.5 and a half-inactivation voltage of about -120 mV.

and c were obtained after prepulses to -100 mV for 250, 1,000, and 2,000 ms, respectively. The longer prepulses to -100 mV resulted in a slower activation time course. In the data shown in Fig. 17B, the activation rates, as measured by the time to reach 50% of the peak probability of the channel being open after 250, 1,000, and 2,000 ms, were ~6.5, 35, and 50 ms.

K_X channels. Fig. 18A shows the ensemble averages of the K_X channel openings recorded at $+50$ mV following 480-ms prepulses to -130 and -70 mV. The K_X channel did not show an appreciable amount of inactivation during a depolarizing pulse but was strongly influenced by the holding voltage (Fig. 18A). Prepulses to -70 mV totally inactivated the channel. The dependence of the channel on the prepulse voltage is shown in Fig. 18B. Prepulses to voltages more negative than -100 mV were required to activate the K_X channel. The voltage dependence data were fitted by a Boltzmann function with an equivalent

charge of 2.5 and a half-inactivation voltage of −120 mV. We do not have detailed information on the voltage dependence of activation of this channel.

K_W *channels.* Fig. 19A shows the ensemble averages of openings of the K_W channels in response to 240-ms depolarizing pulses to −10, +10, and +40 mV.
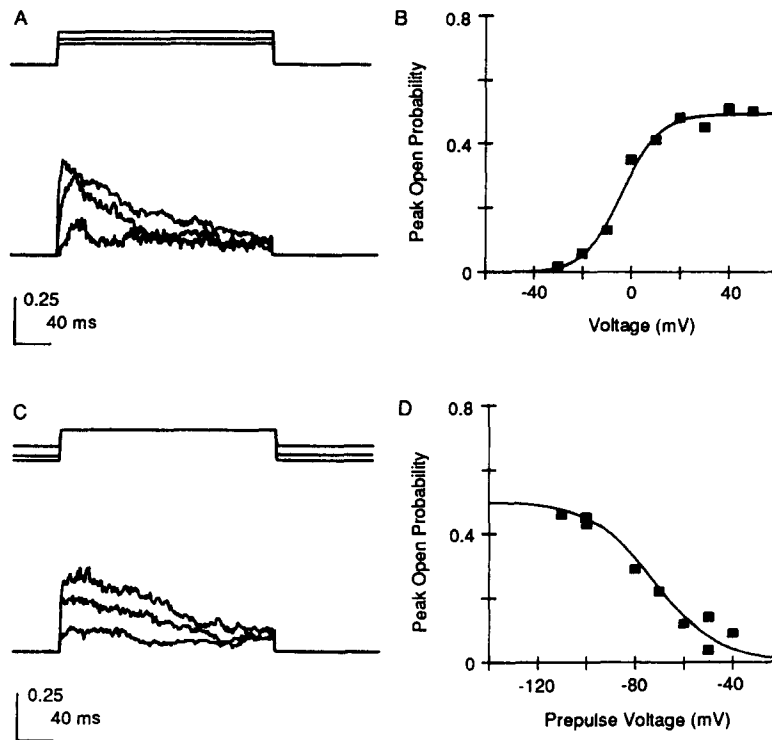

FIGURE 19. Voltage-dependent activation of K_W channels. (A) Ensemble averages of the openings of the K_W channels recorded at −30, −10, and +20 mV (from bottom to top). The patch was depolarized to these voltages after 250-ms prepulses to −100 mV. The holding voltage was −50 mV. Pulses were applied every 5 s. Data were filtered at 1 kHz and sampled at 10 kHz. Ensemble averages were digitally filtered at 400 Hz. (B) Voltage dependence of the peak probability of the channel being open. Openings were elicited as described in A. Data were fitted with a Boltzmann function with an equivalent charge movement of ~3 and a half-activation voltage of 0 mV. (C) Ensemble averages of the openings of the K_W channel recorded at +30 mV after 250-ms prepulses to −40, −70, and −100 mV (from bottom to top). Pulses were applied every 5 s. Data were filtered at 1 kHz and sampled at 10 kHz. Ensemble averages were digitally filtered at 400 Hz. (D) Dependence of the peak probability of the channel being open on the prepulse voltage. Openings were elicited as described in C. The peak probabilities of the channel being open are plotted against the prepulse voltage. Data were fitted with a Boltzmann function with an equivalent charge of 2 and a half-inactivation voltage of −70 mV.

Upon depolarization, the K_W channels activated quickly and inactivated according to a roughly single-exponential time course. The time course of the decline of the probability of the K_W channel being open varied considerably among the patches examined. The time constants were usually between 40 and 80 ms in

the range of 10–50 mV. The records in Fig. 19A show the less transient behavior of the K_W channel and those in Fig. 10A show the more transient. The time course of the decline of the open probability was not markedly dependent on the test voltage at voltages more positive than +10 mV. The steady state probability of the K_W channel being open was negligible.

Fig. 19B plots the peak probability of the channel being open against the test voltage when the holding voltage was −100 mV. The channels started to activate around −30 mV and the probability of being open saturated at +20 mV. This voltage dependence of the probability of the channel being open was fitted by a Boltzmann function with an equivalent charge of ~3 and a half-activation point of 0 mV.

The probability of the K_W channel being open was affected by the prepulse voltage. Fig. 19C shows the ensemble averages recorded at +30 mV following prepulses to three different voltages. Depolarizing prepulses reduced the probability of the channel being open. The dependence of the probability of the K_W channel being open on the prepulse voltage is shown in Fig. 19D. This voltage dependence was fitted with a Boltzmann function with an equivalent charge movement of 2 and a half-inactivation voltage of −70 mV.

The K_W channels were observed only very infrequently in PC-12 cells grown in the absence of NGF. These K_W channels appeared to be observed more frequently in the cell-attached configuration than in the excised configurations, although quantitative comparisons were not made.

DISCUSSION

Kinetically and Pharmacologically Distinct Whole-Cell K^+ Currents in PC-12 Cells

In a majority of the cells, depolarizing pulses elicited whole-cell K^+ currents that activated quickly and declined slowly. Neither the time course nor the peak amplitudes of the currents were steeply dependent on the prepulse voltage. The results of the whole-cell recording do not readily suggest that more than one distinct population of K^+ channel contributed significantly to the whole-cell K^+ currents. The only suggestion that more than one type of K^+ channel contributed to the whole-cell currents was that the voltage dependence of the fraction of the total conductance activated, measured from the tail currents, was different at different times after the pulse termination. The whole-cell current data alone do not substantiate the existence of more than one type of K^+ current in PC-12 cells contributing significantly to the total whole-cell currents. Single-channel recordings show that PC-12 cells have several different classes of voltage-gated K^+ channels.

Transient whole-cell currents. It is not clear whether the transient whole-cell K^+ currents observed in a very small number of cells actually represent A-currents. Traditionally, A-currents have been defined as voltage-dependent K^+ currents that inactivate rapidly with maintained depolarization and have a steep dependence on the prepulse voltage. The transient currents observed in PC-12 cells inactivated rapidly (time constant of inactivation of ~40–80 ms at greater

than +10 mV) and were dependent on the holding voltage (see Fig. 6). On this basis, they could be considered A-currents. However, the transient currents in PC-12 cells are slower and less dependent on the holding voltage than the A-currents observed in other preparations (for review, see Rogawski, 1985). The transient currents were observed only in a very small fraction of the cells examined. If these transient currents had been present in most of the cells examined but were masked by less transient K^+ currents, we should have been able to isolate the transient currents at least partly by manipulating the prepulse voltage. However, as shown in Fig. 1 C, prepulses to a wide voltage range (−130 to −20 mV) did not unmask transient currents. Thus, we conclude that only a small number of PC-12 cells expressed these transient currents in large number, which suggests that the PC-12 cells are not totally homogeneous. Some subclones of PC-12 cells may express certain types of K^+ channels more than others.

Summary of Properties of Four Types of Voltage-dependent K^+ Channels in PC-12 Cells

We described the time course of activation and inactivation of four different types of voltage-dependent K^+ channels in PC-12 cells. Fig. 20 summarizes the time courses of the open probabilities of the four different voltage-dependent K^+ channels and their voltage-dependent activation and inactivation properties. These four types of K^+ channels varied in the time course of macroscopic activation and inactivation. These K^+ channels also differed in their dependence on the holding voltage. The peak probability of the openings of the K_W and K_X channels was very dependent on the holding voltage, whereas that of the K_Z and K_Y channels was less dependent on the holding voltage.

We have interpreted our results as being representative of four distinct classes of K^+ channels. An alternative interpretation would be that there is a single class of channels whose gating consists of transitions between different conductance sublevels and kinetic modes (Jahr and Stevens, 1987; Cull-Candy and Usowicz, 1987). This possibility seems unlikely for the following reasons. All four classes of channels were observed in patches in isolation and in conjunction with members of other classes. The probability of occurrence in a patch and the gating properties of one class of channel are not influenced by other classes of channels in the patch. Within the time course of an experiment (up to 2 h), we did not see channels convert from one class to another. Our results do not address the possibility of slow interconversion of channel types with time courses much longer than a few hours.

Comparison with Previous Studies of Single K^+ Channels

Classification of K^+ channels. Traditionally, K^+ channels activated by depolarization have been classified mainly as A-current channels and delayed rectifier channels (see Rudy, 1987). This classification is based on the macroscopic K^+ currents observed. Delayed rectifiers are those that do not show much inactivation with maintained depolarization and do not depend greatly on the holding voltage. In our study, both K_Z and K_Y channels could qualify as delayed rectifier channels. The time course of the probability of being open of the K_X channel

THE JOURNAL OF GENERAL PHYSIOLOGY · VOLUME 91 · 1988

also resembles that of delayed rectifier channels. However, the very steep dependence of the open probability of the K_X channel on the holding voltage is not typical for the delayed rectifier–type channels.

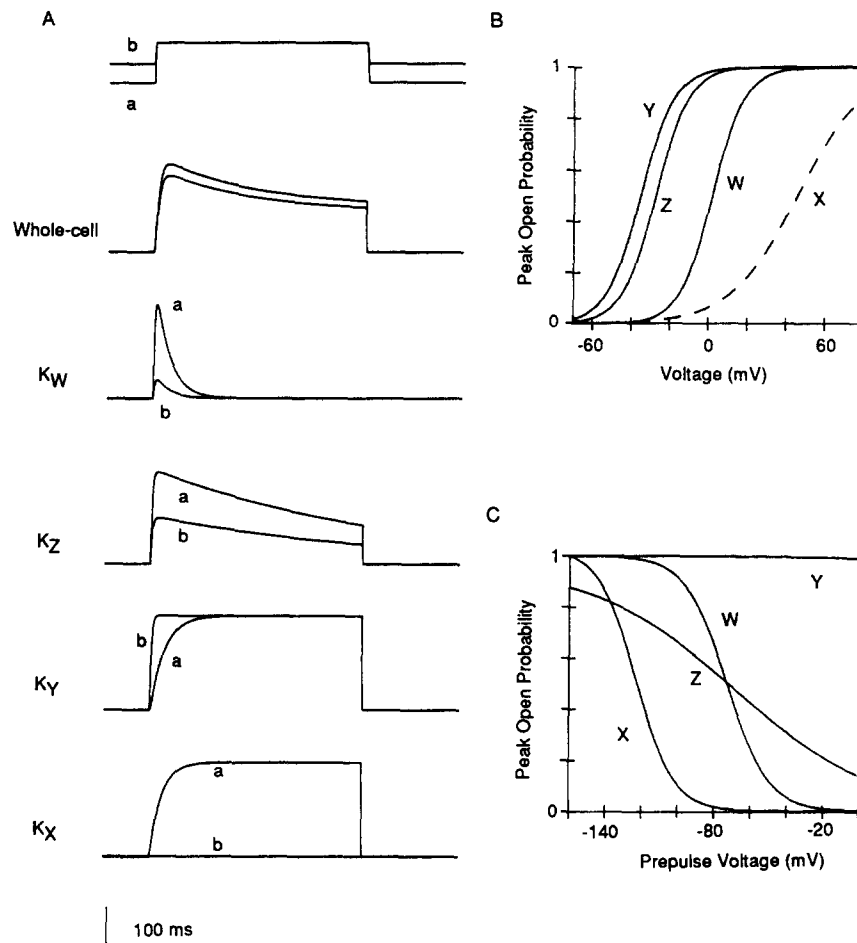*Delayed rectifier channel.* The effects of prepulses on the activation kinetics

FIGURE 20. Summary of voltage-dependent gating of four types of K channels in PC-12 cells. This illustration summarizes the gating properties of the four different types of K^+ channels in PC-12 cells. The sweeps shown are not real data. (A) Comparison of the time course of the whole-cell K^+ currents and the time courses of the probabilities of the channel being open. The top shows the voltage pulse protocol: two voltage pulses to the same voltage (e.g., +20 mV) following prepulses to two different voltages (e.g., −120 and −40 mV). (B) Dependence of probabilities of being open of the four different classes of K^+ channels on the test voltage. The solid lines are based on the experimental data obtained and dotted lines are inferred on the basis of the data obtained at other voltages. (C) Dependence of probabilities of being open of four different classes of K^+ channels on the prepulse voltage.

of the 7-pS K_Y channels are similar to those reported by Cole and Moore (1960) for squid delayed rectifier currents. This suggests that channels similar to the K_Y channels may contribute to the delayed rectifier currents in squid axons. Conti and Neher (1980) showed that a delayed rectifier K^+ channel in squid axon when the K^+ gradient is reversed has a conductance of ~17 pS. It is possible that their higher conductance value is the result of the higher ionic concentration in the squid physiological solution. More recently, Standen et al. (1985) recorded from single K^+ channels presumed to underlie delayed rectifier currents in skeletal muscle cells. They showed that these channels had a conductance of ~15 pS, which is slightly greater than that for the K_Z channel in PC-12 cells. The outward rectifier K^+ channels in mouse macrophages reported by Ypey and Clapham (1984) closely resemble the K_Z channels reported in this study. Both the outward rectifier K^+ channels in macrophages and the K_Z channels inactivated with a very similar time course with a time constant of ~500 ms. These K^+ channels in macrophages had a conductance of ~16 pS.

Transient channels. The time course of inactivation and the dependence of the peak probability of the channel being open for the K_W channels are similar to these properties of the transient whole-cell currents. Furthermore, both the K_W channels and the transient currents were observed very infrequently. Thus, we suggest that the K_W channels underlie the transient whole-cell K^+ current observed in a small number of PC-12 cells. The K_W channels in PC-12 cells are similar to the fast transient K^+ channels of Cooper and Shrier (1985) in nodose neurons and of Kasai et al. (1986) in dorsal root ganglion cells. The transient channels in these neurons have a conductance of 20–22 pS. However, the time constant of the inactivation of the transient channel in rat nodose neuron is ~30 ms, twice as fast as that for the K_W channel reported in this article. The transient channel in dorsal root ganglion cells has a voltage dependence of activation and inactivation similar to that of the transient K_W channel in PC-12 cells, but it has a slower inactivation time course. The voltage dependence of activation and inactivation of the transient K^+ channel in dorsal root ganglion cells is also similar to that of K_W channels in PC-12 cells. The K_W channels are also slower in inactivation time course than the transient K^+ channels termed A_1 channels in cultured *Drosophila* muscle cells (Solc et al., 1987).

Marty and Neher (1985) reported that bovine adrenal chromaffin cells have three types of voltage-dependent K^+ channels. One of the three was the large Ca^{++}-dependent K^+ channel described in PC-12 cells and other cells. Two other types of channels, termed FK and SK channels, were ~12 and 8 pS in conductance. FK channels were transient in time course and SK channels were less transient. Quandt (1987) reported that neuroblastoma cells have two distinct classes of voltage-dependent K^+ channels in addition to the large Ca^{++}-dependent K^+ channels. These K^+ channels had conductances of 35 and 14 pS in symmetrical K^+ solutions. The 35-pS channel was termed the delayed rectifier channel and was blocked by 4-AP. These two types of K^+ channels do not appear to correspond to any of the four types of K^+ channels reported in this study. It is not clear whether any of these K^+ channels correspond to the K_W and K_Y channels in PC-12 cells.

Reconstruction of the Whole-Cell Currents

We suggest that K_Z channels are predominantly responsible for the properties of the whole-cell currents for the following reasons. (*a*) K_Z channels are found most frequently in excised and cell-attached patches, more often than other types of K^+ channels. (*b*) The time course of activation is similar (but not identical). (*c*) The voltage dependence of activation is similar. (*d*) The sensitivities of the whole-cell and K_Z channels to TEA, 4-AP, and CTX are similar. The following observations, however, suggest that other types of K^+ channels also contributed to the whole-cell currents. (*a*) The time course of the inactivation of the whole-cell currents (50% decline in 2–3 s) was much slower than that of the K_Z channels (100–600 ms). (*b*) Whole-cell K^+ currents showed less dependence on depolarizing prepulses. These differences could be explained by assuming that sustained K^+ channels, which do not show much dependence on the holding voltage, such as K_Y, contributed significantly to the whole-cell K^+ currents.

The physiological roles of the K_X channel are not clear. Because K_X channels cannot be activated unless hyperpolarizing prepulses to -120 to -140 mV are given, their physiological roles are probably very limited unless some modulatory agents shift the voltage dependence. In the whole-cell records, however, prepulses to very negative voltages did not reveal any additional currents. Thus, only a small number of K_X channels can be expressed in PC-12 cells.

Modulation and Regulation of K^+ Channels in PC-12 Cells

PC-12 cells have many distinct types of voltage-dependent K^+ channels in large number, which allows the cell to respond to a variety of stimuli in different ways by selectively regulating certain types of K^+ channels. One biologically active agent may have very different actions on different types of K^+ channels. That the inactivation time course of the K_Z channel was variable among the patches examined suggests that the inactivation process could be readily regulated by intracellular factors. The inactivation process of voltage-dependent K^+ channels can be modulated by biologically relevant agents (e.g., Strong, 1984). Long-term regulation of cellular excitability is also possible by changing the relative number of different types of channel proteins expressed. For example, NGF-induced differentiation of PC-12 cells may involve changes in the properties of these K^+ channels and/or the number of these channels expressed by the cells. A K^+ conductance sensitive to apamin appeared to be regulated by NGF in PC-12 cells (Schmid-Antomarch et al., 1986).

REFERENCES

Barrett, J. N., K. L. Magleby, and B. S. Pallotta. 1982. Properties of single calcium-activated potassium channels in cultured rat muscle. *Journal of Physiology.* 331:211–230.

Cole, K. S., and W. J. Moore. 1960. Potassium ion current in the squid giant axon; dynamic characteristics. *Biophysical Journal.* 1:1–14.

Colquhoun, D., and F. J. Sigworth. 1983. Fitting and statistical analysis of single channel records. *In* Single Channel Recording. B. Sakmann and E. Neher, editors. Plenum Publishing Corp., New York. 191–263.

Conti, F., and E. Neher. 1980. Single channel recordings of K⁺ currents in squid axons. *Nature.* 285:140–143.

Cooper, E., and A. Shrier. 1985. Single-channel analysis of fast transient potassium currents from rat nodose neurones. *Journal of Physiology.* 369:199–208.

Cull-Candy, S. G., and M. M. Usowicz. 1987. Multiple-conductance channels activated by excitatory amino acids in cerebellar neurons. *Nature.* 325:525–528.

Dichter, M., A. S. Tischler, and L. A. Greene. 1977. Nerve growth factor-induced and acetylcholine sensitivity of a rat pheochromocytoma cell line. *Nature.* 268:501–504.

Greene, L. A., and A. S. Tischler. 1976. Establishment of a noradrenergic clonal line of rat adrenal pheochromocytoma cells which respond to nerve growth factor. *Proceedings of the National Academy of Sciences.* 73:2422–2428.

Hamill, O. P., A. Marty, E. Neher, B. Sakmann, and F. J. Sigworth. 1981. Improved patch clamp techniques for high-resolution current recording from cells and cell-free membrane patches. *Pflügers Archiv.* 391:85–100.

Hoshi, T., and R. W. Aldrich. 1988. Gating kinetics of four classes of voltage-dependent K⁺ channels in pheochromocytoma cells. *Journal of General Physiology.* 91:107–131.

Hoshi, T., J. Rothlein, and S. J. Smith. 1984. Facilitation of Ca²⁺-channel currents in bovine adrenal chromaffin cells. *Proceedings of the National Academy of Sciences.* 81:5871–5875.

Jahr, C. E., and C. F. Stevens. 1987. Glutamate activates multiple single channel conductances in hippocampal neurones. *Nature.* 325:522–525.

Kasai, H., M. Kameyama, K. Yamaguchi, and J. Fukida. 1986. Single transient K channels in mammalian sensory neurons. *Biophysical Journal.* 49:1243–1247.

Latorre, R., R. Coronado, and C. Vergara. 1984. K⁺ channels gated by voltage and ions. *Annual Review of Physiology.* 46:485–495.

Marty, A. 1983a. Blocking of large unitary calcium-dependent potassium currents by internal sodium ions. *Pflügers Archiv.* 396:179–181.

Marty, A. 1983b. Ca²⁺-dependent K⁺ channels with large unitary conductance. *Trends in Neurosciences.* 6:262–265.

Marty, A., and E. Neher. 1985. Potassium channels in cultured bovine adrenal chromaffin cells. *Journal of Physiology.* 367:117–141.

Miller, C., E. Moczydlowski, R. Latorre, and M. Phillips. 1985. Charybdotoxin, a protein inhibitor of single Ca²⁺-activated K⁺ channels from mammalian skeletal muscle. *Nature.* 313:316–318.

Quandt, F. N. 1987. Three kinetically distinct potassium channels in mouse neuroblastoma cells. *Journal of Physiology.* In press.

Rogawski, M. A. 1985. The A-current: how ubiquitous a feature of excitable cells is it? *Trends in Neurosciences.* 8:214–219.

Rudy, B. 1987. Diversity and ubiquity of K channels. *Neuroscience.* In press.

Schmid-Antomarch, H., M. Hugues, and M. Lazdunski. 1986. Properties of the apamin-sensitive Ca⁺⁺-activated K⁺ channel in PC12 pheochromocytoma cells which hyper-produce the apamin receptor. *Journal of Biological Chemistry.* 261:8633–8637.

Solc, C. K., W. N. Zagotta, and R. W. Aldrich. 1987. Single-channel and genetic analyses reveal two distinct A-type potassium channels in *Drosophila. Science.* 236:1094–1098.

Standen, N. B., P. R. Stanfield, and T. A. Ward. 1985. Properties of single potassium channels in vesicles formed from the sarcolemma of frog skeletal muscle. *Journal of Physiology.* 364:339–358.

Strong, J. A. 1984. Modulation of potassium current kinetics in bag cell neurons of *Aplysia* by an activator of adenylate cyclase. *Journal of Neuroscience.* 11:2772–2783.

Thompson, H., and R. W. Aldrich. 1980. Membrane potassium channels. *In* The Cell Surface and Neuronal Function. C. W. Cotman, G. Poste, and G. L. Nicolson, editors. Elsevier/ North-Holland, New York. 49–85.

Yellen, G. 1984. Ionic permeation and blockage in Ca^{2+}-activated K^+ channels of bovine chromaffin cells. *Journal of General Physiology.* 84:157–186.

Ypey, D. L., and D. E. Clapham. 1984. Development of a delayed outward-rectifying K^+ conductance in cultured mouse perotoneal macrophages. *Proceedings of the National Academy of Sciences.* 81:3083–3087.